Influence of low – structure carbon black on the electrical, rheological and mechanical properties of graphite nanoplatelets/ethyl butyl acrylate composites

A study of the effects of low – structure carbon black on the electrical, mechanical and rheological behaviors of graphite nanoplatelets/ethyl butyl acrylate composites for applications in high voltage power cables

by

GIAMPAOLO ARIU

Diploma work No. 105/2013
at Department of Materials and Manufacturing Technology
CHALMERS UNIVERSITY OF TECHNOLOGY
Gothenburg, Sweden

Diploma work as an Erasmus exchange student

Performed at: Department of Materials and Manufacturing Technology
Chalmers University of Technology, SE - 412 96 Gothenburg

Supervisor: Henrik Oxfall
Department of Materials and Manufacturing Technology
Chalmers University of Technology, SE - 412 96 Gothenburg

Examiner: Professor Mikael Rigdahl
Department of Materials and Manufacturing Technology
Chalmers University of Technology, SE - 412 96 Gothenburg

Influence of low – structure carbon black on the electrical, rheological and mechanical properties of graphite nanoplatelets/ethyl butyl acrylate composites
- A study of the effects of low – structure carbon black on the electrical, mechanical and rheological behaviors of graphite nanoplatelets/ethyl butyl acrylate composites for applications in high voltage power cables.
GIAMPAOLO ARIU

Diploma work no 105/2013
Department of Materials and Manufacturing Technology
Chalmers University of Technology
SE-412 96 Gothenburg
Sweden
Telephone + 46 (0)31-772 1000

[CTH REPROSERVICE]
Gothenburg, Sweden 2013

Influence of low – structure carbon black on the electrical, rheological and mechanical properties of graphite nanoplatelets/ethyl butyl acrylate composites

- A study of the effects of low – structure carbon black on the electrical, mechanical and rheological behaviors of graphite nanoplatelets/ethyl butyl acrylate composites for applications in high voltage power cables.

GIAMPAOLO ARIU

Department of Materials and Manufacturing Technology

Chalmers University of Technology

Abstract

The semiconductive layers employed for manufacturing power cables are typically composed of a polymer matrix filled with conductive fillers. The aim of this work has been to assess the influence of the filler loadings into a polymer matrix, ethyl butyl acrylate (EBA), such as low – structure carbon black (LS – CB) and exfoliated graphite nanoplatelets (GNPs) GNP not xngp, on the electrical, rheological and mechanical properties of the composite. The attention was focused on a possible *synergistic effect* between the fillers, in order to create hybrid systems (characterized by GNP/LS – CB repartitions of 80/20, 70/30 and 60/40) with enhanced properties. Electrical, rheological and mechanical (uniaxial tensile) tests were performed on specimens extruded at 2 mm/min or 20 mm/min, with the hybrids showing an increased electrical conductivity σ and tensile modulus of the composite E_c with an increasing filler volume content. The electrical percolation threshold was in most cases lower for the hybrid systems than for the pure GNP – EBA system, although the *rheological percolation threshold* increased slightly (as suggested by the behavior of the storage modulus G' as a function of the frequency (Hz) used during the dynamic tests).
A microstructural analysis using SEM (Scanning Electron Microscope) revealed an orientation of the filler particles given by the extrusion which, when performed at higher speed (20 mm/min), also affected the electrical conductivity and the tensile modulus E_c (MPa), both decreasing.
The tensile modulus results were also analyzed in terms of the Nielsen and Halpin – Tsai models, whose performances were compared at a fixed tensile modulus of the filler E_f. The main attention was paid to the Nielsen fitting model, which appeared to provide a better prediction of the experimental results.

Keywords: ethyl butyl acrylate (EBA), low – structure carbon black (LS – CB), exfoliated graphite nanoplatelets (GNP), hybrid systems, percolation threshold, electrical and rheological properties, tensile tests.

Contents

Acknowledgements

This master degree thesis has been carried out from September 2012 to January 2013. The experimental tests have been conducted at the Department of Materials and Manufacturing Technology at Chalmers University of Technology.

The work has been done with the precious help and support of the people working at the department. I would like to thank directly them, and in particular my examiner, Prof. Mikael Rigdahl, for giving me the opportunity to perform my thesis at this prestigious university, and my academic supervisor, Henrik Oxfall, for being always available for improving my practical and theoretical knowledge, giving me his support and guidance during the entire laboratory project.

Göteborg January 2013

Giampaolo Ariu

Abbreviations

2HEA	2 ethyl hexyl acrylate
BET	Brunauer, Emmet and Teller
CAN	Controller area network
CB	Carbon black
CNTs	Carbon nanotubes
DBPA (DBP)	Dibutylphthalate absorption
EBA	Ethyl butyl acrylate
EMA	Ethyl methyl acrylate
GIC	Graphite intercalation compounds
GNP	Graphite nanoplatelets
GO	Graphite oxide
HDPE	High density polyethylene
HS – CB	High – structure carbon black
LLDPE	Linear low density polyethylene
LS – CB	Low – structure carbon black
NMP	N – methylpyrrolidone
PC	Propylene carbonate
PE	Polyethylene
PIPS	Precision ion polishing system
PP	Polypropylene
SEM	Scanning electron microscope

1. Introduction

Power cables are composed of a semiconductive polymeric layer (termed *conductor screen*), used to limit and homogenize the electromagnetic field, preventing the risk of an electric breakdown. This is typically made of polyethylene or related copolymers, and placed between the conductor and the insulation (the latter covered with another semiconductive layer, known as *insulation screen*, as shown in **Figure 1**).

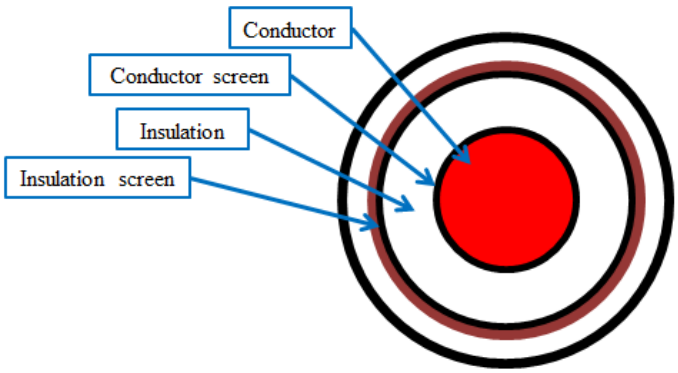

Figure 1. The structure of a high voltage power cable.

The semiconductive layers commercially used are typically charged with a huge amount of conductive filler, usually carbon black CB, at high weight concentrations, up to or above 40 weight - % (wt%). The aim of several studies has been the optimization of the filler loadings, in order to reduce their negative influence on the mechanical, electrical and rheological performances. The present and future purpose is to find alternative conductive nanofillers, even remembering the issue concerning the electrical insulation. For this reason, the first attentions were focused on graphene and polymer nanocomposites containing this material. In the last years, many works have been devoted to that, as reported in the literature **[1, 2, 3, 4]**.

Subsequently, it has been found that a combination of different types of fillers, mostly carbonaceous, can bring relevant improvements, especially on the electrical, mechanical and rheological properties, with the so – called *synergistic effect*. The work by **Via *et al.* [5]** showed the existence of this phenomenon, studying several systems with a mixture of CNTs (carbon nanotubes), CB (carbon black) and GNPs (exfoliated graphite nanoplatelets). They showed a decrease of the electrical parameter known as the *percolation threshold*, and even the viscosity of the composite, if compared to single filler composite at the same filler contents.
Most of the works in the scientific literature refer to a particular type of carbon black, high – structure HS – CB. This work focuses on the low – structure type, and its influence on electrical, mechanical and rheological performances, once added to systems composed of EBA (ethyl butyl acrylate copolymers) as the polymer matrix (commercially chosen for electrical purposes in power cables fabrication) and GNPs (exfoliated graphite nanoplatelets) as the carbonaceous filler.
A compounding process of the starting materials has been performed with two Brabender mixing chambers, in order to obtain the specimens of pure GNP or pure LS – CB in EBA, and their hybrids, being analyzed electrically, mechanically and rheologically.

Microstructural studies were performed using the SEM (Scanning Electron Microscope) technique, in order to focus the attention to the effects given by the orientation and the mixing process with respect to the dispersion of the fillers and their distribution in the polymer matrix. Regarding the hybrids, it will be noticed an improvement of the electrical properties given by the already mentioned *synergistic effect* between the fillers will be noticed.
The influence of the extrusion speed from a capillary viscometer on all the properties aforementioned, and therefore of the orientation of the fillers, will be investigated. In particular, the electrical conductivity σ (S/cm) as a function of the filler volume content (volume - %, vol%), and the electrical percolation threshold (vol%) were studied, in parallel with the rheological percolation threshold (vol%). The latter parameter will be obtained from the graphs showing the behavior of the storage modulus G' (MPa) as a function of the frequency (Hz) used during the dynamic tests.
A quick analysis of the influence of different steps of extrusion on the electrical and tensile performances of the composites will be reported.
Uni – axial tensile tests were performed for reporting the behaviors of the tensile modulus of the composite (MPa) and the strain at break (%) as a function of the filler volume fraction (vol%).

The experimental tensile results were analyzed using the Nielsen and Halpin – Tsai models, fixing a value for the tensile modulus of the filler E_f.

The last step involved a more careful study of the first model (Nielsen) mentioned above, by varying alternatively the Einstein coefficient K_E (dependent on the filler geometry) and the tensile modulus of the filler E_f.

1.1 Objective/aim

The aim of this work is to investigate the influence of an addition of low – structure carbon black LS – CB to a composite system made of a polymer matrix EBA filled with exfoliated graphite nanoplatelets GNPs, in terms of electrical and rheological percolation thresholds (in vol%, and their correlations), electrical conductivity σ (S/cm), mechanical properties such as tensile modulus of the composite E_c(MPa) and strain at break (%).

In particular, it will be studied how the *synergistic effect* between the fillers can improve the properties listed above, even regarding materials obtained after several extrusion steps and using two different extrusion speeds (2 mm/min and 20 mm/min), affecting the orientation of the filler particles. Concerning the last purpose mentioned, a microstructural analysis by SEM (Scanning Electron Microscope) was also performed.

2. Theoretical background

2.1 Ethylene acrylic ester copolymers

Ethylene acrylic ester copolymers can be divided into three product families according to the type of acrylic substitution: butyl acrylate (EBA copolymer), methyl acrylate (EMA copolymer) or 2 ethyl hexyl acrylate (2HEA).

The main properties and benefits of ethylene acrylic ester copolymers are the excellent thermal stability, the great adherence to many substrates (like polyethylene, polystyrene, polypropylene and many others), the good chemical resistance, the good elastic properties and the excellent mechanical behavior at low temperatures (for applications such as frozen food packaging, hot – melts have to maintain high level of adhesion and flexibility at -40 °C, known as good *deep – freeze* resistance; the flexibility of an ethylene copolymer based hot – melt is highly linked to its glass transition temperature T_g, preferably as low as possible for the deep – freeze performances). These qualities make them suitable for many applications, including packaging or disposables for example. The chemical structure of ethyl butyl acrylate is shown in **Figure 2**. Thanks to the maleic anhydride or glycidyl methacrylate and their polarity, monomers can react with other functions in order to create chemical bonds, which can increase the resulting adhesion, heat resistance or long term ageing properties. Acrylic esters decrease the crystallinity of the polymer (i.e. polyethylene), which guarantees a wider operating window of the adhesive.

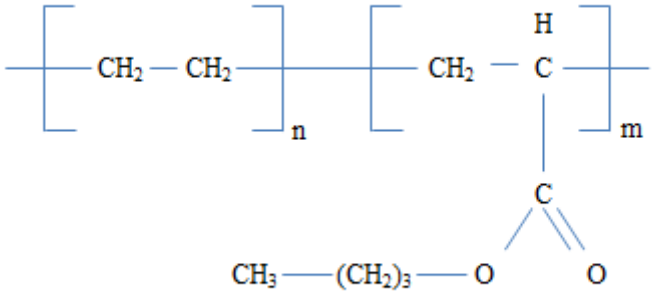

Figure 2. The chemical structure of ethyl butyl acrylate copolymer (EBA).

2.2 Low – structure carbon black (LS – CB)

Carbon black is made of small functional units called *aggregates*. They are generated thanks to the fusion of smaller units, named *primary particles*, in order to form a three dimensional branched chain structure **[6]**. Aggregates are connected each other by Van der Waals forces holding sheets together, and are more or less unbreakable **[7]**.

Carbon black is mainly produced using two dominant processes: the oil – furnace black process and the thermal black process **[7, 8]**.

The oil – furnace process guarantees the partial combustion of residual aromatic oils into a high temperature (1400 – 1800 °C) reactor, with the aim of cracking and dehydrogenating the hydrocarbon, resulting in a carbon with a pseudo – graphitic microstructure. The most common feedstock is decanted oil from gasoline **[7]**. In order to remove the gases contained

into the carbon black, a double quench with water is used, and then the material is filtered to separate the unagglomerated carbon black **[7]**. In the reactor, the fusion of the primary particles can be controlled to obtain different degrees of clustering. Grades optimized for plastics use a special manufacturing technology for improved dispersion and other critical properties to enhance specific performances depending on the applications.

The thermal black process is characterized by decomposition of natural and coke oven gases, or liquid hydrocarbons in the absence of air **[7]**, and it allows the production of coarse carbon black. This process, conducted at high temperatures, produces carbon black, hydrogen, methane, and other hydrocarbons.

The aggregate size of CB depends on the grade, each having its own mean aggregate size, generally in the range of 0.01 – 1 μm. Despite the small size of the aggregates, carbon black can include a limited fraction of smaller materials, known as nano – scale materials.

Low – structure carbon blacks (LS – CB) are typically less easily dispersed than high – structure carbon blacks (HS – CB) of similar surface area. A high – structure carbon black is characterized by aggregates composed of many primary particles, clustered together with considerable branching and chaining. As a result, the aggregates pack more poorly reducing the inter – aggregate attractive forces. Low structure carbon blacks are more compact, allowing closer packing and greater attractive interactions. For this reason, the dispersion is more difficult. However, the higher density of low – structure carbon black allows it to incorporate easier into the polymer matrix since there is less occluded air to displace, even though it needs more energy to be dispersed.

An oil absorption process, called *dibutylphthalate absorption* (DBPA or DBP **[9]**), allows to indicate the structure of carbon black. Indeed, it is possible to distinguish a high – structure carbon black from a low – structure one by its higher oil absorptions. Another feature which depends on the type of carbon black analyzed is the blackness, the so – called *masstone* **[10]**, and it is higher for the low – structure carbon black.

Carbon black shows the first signals of a decomposition between 450 to 500°C under air or oxygen. At the same temperature conditions, a nitrogen atmosphere does not cause decomposition of carbon black.

Carbon black adsorbs moisture up to an equilibrium absorption value, typically reported as a weight percentage (wt%). This value varies depends on the grade of the carbon black, therefore on the surface area and the surface chemistry.

One of the important parameters used to estimate the market price of the carbon black is the volatile content, meaning the number of oxygenous groups on the surface. This parameter has a relevant influence on the electro - chemical performance and applications. **Table 1** shown below summarizes the main physical and chemical differences between low – structure LS and high – structure HS carbon black **[7, 9, 10]**.

Table 1. Main differences between low – structure LS and high – structure HS carbon black **[7, 9, 10]**.

Property	Low structure carbon black LS – CB	High structure carbon black HS – CB
Adsorption	Low	High
Viscosity	Low	High
Color darkness	High	Low
Dispersivity	Difficult	Easy

A large amount of carbon black is used mainly in tires as excellent rubber reinforcement. This material is also an excellent coloring agent as being black pigment, and therefore is widely used for printing inks, resin coloring, paints, and toners.
Furthermore, carbon black is used in various other applications as an electrically conductive agent, including antistatic films, fibers, and floppy disks.

2.3 Exfoliated graphite nanoplatelets (GNP)

Graphite is a carbonaceous material characterized by covalent bonds between the sp^2 – hybridized carbon heteroatoms, organized in individual graphene one – atom – thick layers **[11]**. These structures have a hexagonal shape, and form stacks thanks to Van der Waals interactions between them. Their relevant mechanical and thermal properties, such as the high aspect ratio and the stiffness of the graphene sheets (around 1 TPa, as shown for carbon nanotubes CNTs), the excellent thermal and electrical conductivity (around 3000 W/(m K) and 10^6 S/cm, respectively), suggest their use and effective dispersion into polymer matrices **[12, 13]**.

In order to achieve this goal, a precursor needs to be used, such as graphite intercalation compounds (GICs) and graphite oxide (GO). This can guarantee a good exfoliation of the graphite and a more effective dispersion into a polymer matrix.

Regarding GICs, these are composed of graphite with alkali metals or mineral (sulfuric and nitric) acids between the graphene sheets mentioned previously. Their aim is to ensure a weakening of the Van der Waals interactions between the different carbon layers, bringing an increase of the interlayer spacing. The expected effect is the facilitation of the exfoliation of the GIC.

The alternating distribution of the graphene and intercalant layers can affect the exfoliation process positively.

The following step consists in a possible rapid heating or microwave treatment **[14]**, which can guarantee an easier augment of the distance between the layers, not completely separated yet. The resulting material is known as Expanded Graphite (EG), which can be slightly

oxidized by the acid treatment. They are characterized by a limited surface area (around 40 m^2/g) and the layered structure. They are not useful in order to maximize the mechanical properties of a polymer matrix: hence, an exfoliation step is required.

Alternatively, a micro – mechanical procedure, without using intercalants can be used. Possible treatments such as sonication of graphite layers in water, their direct exfoliation into solvents (e.g. propylene carbonate PC or N – methylpyrrolidone NMP) or electrochemical exfoliation in ionic liquids, have been reported in several works **[15, 16, 17]**, but still there is a need of a more focused analysis and application.

Graphite can be treated with $KMnO_4$ and H_2SO_4, or $KClO_3$ and HNO_3, according to Hummers and Staudenmaier or Brodie methods, respectively. The purpose is to guarantee the implantation of oxigeneous chemical functionalities into its structure, for example epoxy or hydroxyl groups on the basal plane and carboxylic acid ones on the edges of the graphene layers **[18]**, more distant than in the untreated graphite structure because of the intercalation of humidity during the oxidation process **[3]**.

The exfoliation of GO can be obtained with several techniques, such as solvent – based and thermal treatments. The first involves the mechanical exfoliation, with stirring or ultrasonication, into water (where GO can be well dispersed thanks to the hydrophilic oxygeneous groups) of at maximum 3 mg/ml of GO, generating a suspension of well separated layers of GO. The second is referred to as a heating shock process, conducted in a quartz tube or vessel, which causes a quick expansion of the structure, and the increasing pressure can bring microstructural changes. The heating rates can reach values of 2000 ˚C/min, up to 400 ˚C. Once the colloidal suspensions of GO, also named G – O, are created, these need a pH stabilization, in order not to create agglomerates of graphite platelets due to a reduction treatment, and this can be done in organic solvent or water **[3]**.

The final step involves reductant agents, for example hydrazine monohydrate or sodium borohydride, with the aim of ensuring the evolution of the separated oxidized layers to graphite nanoplatelets (GNP) **[3, 18]**.

Once exfoliated and expanded, the graphite platelets can be introduced into the polymer matrix via several procedures, such as solvent mixing and in – situ polymerization.

2.4 Capillary viscometers

In order to study the behavior of the composite, the objective of this thesis, in terms of force required for its deformation and the properties of flow of matter, the most useful science is the rheology (from the Greek, *panta rei* = all things flow). The deformation is known as the relative displacement between two points in a sample, and it could be divided into two categories, flow and elasticity.
The former concept concerns the irreversible part of deformation, meaning the material does not recover its original configuration after the removal of the stress applied. In this case the work is converted into heat. The latter category pertains to the reversible part of deformation, when the sample is able to revert almost completely into the original configuration once the stress is removed: this means that the work is recovered.
The definitions of irreversible and reversible parts of deformation, and their combination, known as viscoelasticity, are largely employed in order to estimate the rheological behavior of the materials.
The study of this topic began in the seventeenth century with Hooke and Newton, and their laws of elasticity for the former and viscous flow for the latter. The first viscous model was

published in the nineteenth century, and it was referred to a flow in a round tube. The first practical application in terms of machine was shown in 1890 with the rotational viscometer. Based on these discoveries, several studies have been performed, with the perspective of including different types of techniques to characterize the rheological response of a liquid subjected to a mechanical stress.

The rheological characterization of viscoelastic materials is a tough procedure, and it requires a careful choice of the viscometer, influenced by some factors. In order to pursue the aim of the study, the shear viscosity function must be correlated to other techniques such as creep, relaxation and sinusoidal oscillatory stress experiments to have a more reliable database of characterizing results. Even the polymer processing parameters must be taken into account during the materials characterization, for example molding temperature in injection molding and extrusion pressure during extrusion processes. These factors need an optimization, which could ensure the quality of the analysis.

As mentioned, the choice of the viscometer is a very important factor before starting the rheological characterization of the materials. During this step, there are several points to be considered. One of them is the nature of the material going tested, in terms of viscosity, elasticity and their temperature dependence. Another criterion concerns the accuracy and the precision of the testing equipment: academically it influences the research measurements, whereas a quality control must be performed for industry requirements.

Typically the viscometers can guarantee single – point measurements, meaning a single point for each run of the test, not a wide range of results of viscosity or shear stress referred to different shear rates. This fact is very important for non – Newtonian polymer melts because of the shear rate dependence of the viscosity (which remains constant with the shear rate for the Newtonian ones). The viscosity is strongly dependent on the temperature, which needs a careful control. If the temperature control is not performed well, the materials can reveal a thixotropic or shear – thinning behavior, especially in the case of high viscosity and high shear rates of the processing step. If the pressure used during the process on the melt reaches a high value, it must be controlled, becoming a significant criterion being considered.

The main kinds of viscometer, used depending on the specific application, are three: rotational, capillary and moving body ones. Nevertheless, only the first two types will be considered here.

In the rotational rheometer, the fluid being tested separates two basic parts. The most used configuration is the cone – and – plate. A cone rotates against a flat stationary plate with a so – called *gap angle* lower than 3° and, as already mentioned, the tested fluid is between them. The system may be heated in order to estimate the melt viscosity. A schematic representation of a cone – and – plate viscometer is shown in **Figure 3**.

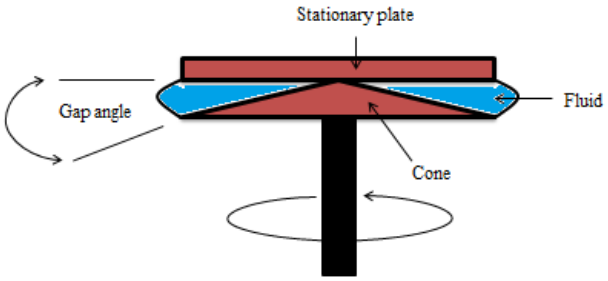

Figure 3. The schematic representation of a cone – and – plate rheometer.

This rheometer permits to gather experimental results on the shear and dynamic components rapidly. The configuration shown can be changed in case of simulations of different flows, like torsional one between parallel plates or *Couette* flow between co – axial cylinders.
The equations **1** and **2** employed to estimate the shear rate $\check{\Upsilon}$ (in s^{-1}) and the stress τ (in Pa) are as follows:

$$\check{\Upsilon} = \frac{\omega_0}{\Omega} \qquad \textbf{[1]}$$

$$\tau = \frac{3 \cdot M}{2 \cdot \pi \cdot R^3} \qquad \textbf{[2]}$$

where ω_0 is the angular velocity (as constant value), Ω the *gap angle*, M the torque and R the cone radius.
The configuration presented above has as advantages a homogeneous shear rate, an easy conversion of the experimental data from the tests and a small size for the samples tested. Experimental difficulties can be that the solvent can evaporate easily, the material can get off of the gap between the cone and the plate, and at high shear rates heating problems can occur, bringing thermal degradation.
The capillary viscometer is the oldest and the most used testing machine for rheological measurements. It is also called *extrusion rheometer*, because of the configuration shown in **Figure 4**.
Extrusion rheometers are generally employed in order to measure melt viscosity of polymers. In **Figure 4** a single hole capillary viscometer is shown, where a plunger moves inside a cylinder of hardened steel at constant speed. The hole is composed of a capillary die at the bottom, characterized by a length L_c and a diameter
$2R_c$. The cross sectional area of the capillary is A_c. These three parameters are fixed before the tests, depending on the polymer and the degree of accuracy desired for the measurements. The test temperature is chosen and maintained thanks to heated blocks around the cylinder. The value is typically fixed between 20 °C and 350 °C.
On the top of the plunger, a load cell is placed, in order to measure the force required to extrude the tested sample through the capillary, maintaining the extrusion speed at a constant value.

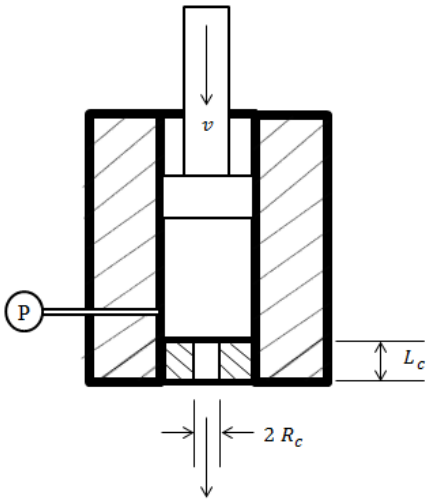

Figure 4. Schematic representation of a capillary viscometer.

Multiple – point measurements can be obtained by setting different extrusion speeds and recording the values of the piston force, readable thanks to a display. In order to reduce the testing time, a multi – bore capillary viscometer can be employed.
There is a consistent difference between the apparent measured values and the corrected ones of the rheological parameters being measured, meaning shear stress τ_W (in Pa), shear rate $\check{\Upsilon}_W$ (in s^{-1}) and viscosity μ_A (in Pa · s). The apparent values are listed below:

$$\tau_W = \frac{\Delta p \cdot R_c}{2 \cdot L_c} \qquad \textbf{[3]}$$

$$\check{\Upsilon}_W = \frac{4 \cdot Q}{\pi \cdot R_c^3} \qquad \textbf{[4]}$$

$$\mu_A = \frac{\tau_W}{\check{\Upsilon}_W} \qquad \textbf{[5]}$$

where Q is the fluid volume flow rate, equal to $A_c \cdot v$ (v is piston speed, in mm/min), F is piston force (in daN), Δp is the ratio between F and A_c, and it is equal to the pressure drop throughout the capillary.
It is possible to use two different corrections for the parameters explained above: the *Bagley* and the *Rabinowitsch correction*. The first accounts for the pressure losses at the entrance and at the exit of the capillary. If non Newtonian fluids are tested, it is possible to get a more accurate estimate of the shear rate by applying the *Rabinowitsch correction*, through a proportionality factor between corrected and apparent value.
The corrected values are listed below:

$$\tau_{corr} = \frac{\Delta p}{2 \cdot \left(\frac{L}{R_c} + e\right)} \qquad \textbf{[6]}$$

$$\check{\Upsilon}_{corr} = \frac{(3 \cdot n + 1)}{4 \cdot n} \cdot \check{\Upsilon}_W \qquad \textbf{[7]}$$

$$\mu_{corr} = \frac{\tau_{corr}}{\check{\Upsilon}_{corr}} \qquad \textbf{[8]}$$

where n is the power law index and e is the Bagley correction, already mentioned previously. The power law index n can be calculated from the slope (n-1) of a plot with apparent viscosity against shear rate, whereas e can be estimated from a Bagley plot.
The shear rates typically found during polymer processing are between 1 and 10 s^{-1} for compression molding, between 10 and 100 s^{-1} for calandering, in the range 100 – 1000 s^{-1} for extrusion and between 1000 – 10000 for injection molding.

2.5 Electrical percolation theory

This theory is largely employed in order to describe the correlation between the dispersion conditions of the filler, particle size and aggregate structure, and the electrical properties (in particular the electrical conductivity) of the composites containing the filler.

Percolation plays an important role in several fields of physical characterization of the composites. The most interesting topic of study related to the electrical analysis is its influence on the conductivity.

The electrically conductive filler is not able to conduct electricity from one side of a composite sample to the other one if the particles are mixed into a polymer material at low concentrations.

The typical polymer matrix used for fabricating the composites has an infinite electrical resistivity: this fact does not allow the whole composite to exhibit a high electrical conductivity unless a path of links of filler particles is created. An increase of filler volume concentration could lead to an improvement in conductivity, thanks to a higher number of links and paths between the particles, which get closer to each other. The volume fraction of filler can be named *percolation threshold* only when the electric conductivity begins to increase considerably. After this, the conductivity may exhibit a plateau behavior, which represents a lower influence of the links between particles.

A way to describe the correlation between the electrical conductivity and the filler content in the region next to the percolation threshold is the following one:

$$\sigma = \kappa(w - w_c)^{\beta} \qquad \textbf{[9]}$$

where σ is the electrical conductivity of the composite, w the filler volume content, w_c the filler volume content at the percolation threshold, κ and β are fitting parameters **[19]**.

Here β is in the range from 1 to 3, depending on the type of the percolation. Instead κ could be connected to the electrical conductivity of the filler, but it is important to recognize that the conductivity of the filler particles does not affect the conductivity of the composite when present at low weight fractions. Their influence begins to be relevant at higher filler contents, becoming the most important parameter for evaluating the conductivity of the composite. For this reason, κ - parameter values cannot be truly related to the conductivity of the filler.

The percolation threshold also hinges on the shape of the filler particles, and it decreases when the length to diameter ratio l/d, and therefore the surface area, of the particles increases. This parameter can obviate the high resistance between the filler particles at low loadings, as typical for the carbon nanotubes CNTs, even thanks to an effective method of dispersion.

In order to further describe the theory of percolation a square lattice composed of different sites, which may have a probability p of being occupied, can be considered. Depending on the occupation, the sites can have very different physical properties. For instance, occupied sites may be represented as conductive ones, whereas empty sites may be considered as insulating ones. The electrical current can flow between nearest – neighbor conductor sites **[6]**.

If the concentration of conductor sites p is low, they are either isolated or agglomerated to form clusters of nearest – neighbor sites. The condition that allows the electrical current to flow between two conductor sites is that these ones belong to the same cluster, meaning when these sites are connected by a path of nearest – neighbor conductor sites. When the concentration p is low, a path like this does not exist, and the mixture is an insulator. At

higher p concentrations, the opposite edges of the lattice can be connected by a large number of conductive paths, in order to guarantee the conduction of the electricity. In this case the mixture behaves as a conductor. Analyzing the intermediate concentrations, it is possible to identify a critical one, typically named *percolation threshold* p_c, where the electrical current begins to percolate from one edge to the other of the lattice: above it the mixture is a conductor, below it behaves as an insulator.

This particular concept of percolation threshold is well referred to a geometrical phase transition, with large clusters in the region distinguishable because of the p_c value. Below p_c only small clusters can be found in the lattice, and their size increases with the value of p. When p reaches its critical value, a large cluster named *infinite cluster*, which connects the two edges of the lattice, exists.

As easily guessable, the critical concentration p_c depends on the features of the lattice, and increases with the decrease of the coordination number and the increase of the size of the lattice (considering the coordination number as constant), due to the weaker entity of the connections between the filler particles and to the wider and more opened structure of the lattice. The triangular lattice, with a coordination number z of 6, has p_c = 0.5, whereas for the square lattice z = 4 and p_c = 0.6, and for the honeycomb lattice z = 3 and p_c = 0.7. The coordination number is 6 for both the triangular and the simple cubic lattice, but the critical composition p_c for the latter lattice is smaller (p_c = 0.3) **[6]**.

2.6 Rheological percolation theory

Polymer nanocomposites can be defined as a mixture of different interacting phases, the polymer matrix and the solid phase as the filler. The system has a nanometric size in at least one dimension.

The two phases can have several degrees of connectivity, and this allows to estimate the nanocomposites as zero – dimensional, one – dimensional, two – dimensional and three – dimensional systems **[20]**.

The zero – dimensional composites are composed of isolated nanofillers in an uninterrupted polymer matrix. The one – dimensional system has nanotubes as loadings, whereas in the two – dimensional composite it is possible to find exfoliated filler layers. The last typology of composite, the three – dimensional one, is characterized by network made of filler particles, with different degree of interconnection.

In particular, the two – dimensional nanocomposites can be classified, hinging upon the nature of the loading, in immiscible systems, intercalated (where the filler layers are separated by the polymer macromolecules) and exfoliated ones (where the individual filler layers are completely disconnected and well dispersed throughout the polymer matrix).

All these systems can be represented by common features, which have relevant influences on the mechanical and rheological performances, such as the nanofiller dispersion throughout the polymer matrix and its content, shape, size and the nature of the connections between the filler particles, also termed *interparticle affinity*. A considerable role is also played by the interfacial effects, meaning the interactions between the particles and the polymer matrix **[20]**.

The first two factors listed above are interconnected, because a good dispersion of the filler throughout the matrix can ensure an improvement of both mechanical and electrical

properties, with a relatively low volume filler fraction. The main reason of this effect is the increased functional surface area.

Depending on the filler volume fraction, the composite can behave in two different ways, the liquid – like and the solid – like behaviors. The first situation manifests at low filler contents, and in this case the storage modulus G' is lower than the loss modulus G''. When the filler content increases, the system acts as a pseudo – solid – like one, and the *cross – over* of the dynamic moduli can be found, meaning the storage modulus G' exceeds the loss one G''. When it happens, a transition limit can be introduced as a describing parameter, called the *rheological percolation*, in parallel with the electrical threshold which represents a change in the electrical conductivity trend (from an insulating system to a conductive one). Nevertheless, in this case the material cannot be considered as a real solid since the modulus is not as high as that of a solid. This response is noted at low frequencies and due to the formation of physical links or percolating network of the filler particles or layers (depending on the filler nature). Consequently, an incomplete relaxation of the polymer chains can be discovered.

As explained above, the interfacial effects between the nanofiller particles and the polymer matrix can bring about the formation of an important network, which manifests in two different ways, the *crowding* and the *chain entanglements*.

The first situation is typical of composites charged with filler particles, whereas the second depends upon the nature of the connection between the macromolecular chains and the filler surfaces. These factors also play a role in influencing the rheological percolation mentioned previously.

In the overview by **Kotsilkova [20]** an example concerning the smectite/epoxy composite system is presented. The main result is the change of the behavior manifested by the composite from liquid – like to pseudo – solid – like with an increase of the smectite content, and the *cross – over* of the dynamic moduli (also because of the high anisotropy of the smectite layers). Regarding the same composite system, according to another rheological method of analyzing the distribution of the filler throughout the matrix, an existence of two rheological percolation thresholds, the *flocculation* and the properly named *percolation* ones, indicated by φ^* and φ^{**} respectively, was found. The *flocculation threshold*, present at low filler content, refers to the formation of clusters of filler particles, with viscous liquid – like behavior, with the storage modulus G' lower than the loss modulus G''; whereas the effective *percolation threshold*, at higher filler amounts, is related to a connection between the clusters, in order to form a continuous network. In this second case, a pseudo – solid – like behavior is shown, and G' exceeds G'' [**20]**.

2.7 Two – point technique for electrical measurements

The two – point technique measures the electrical resistivity (reciprocal of the electrical conductivity) of a material by using the physical dimensions of a standard sample, taken as a rectangular bar with length l, height h and width w. As shown in **Figure 5**, both the two edges of the sample are connected with copper wires, and this gives the name to the experimental technique.

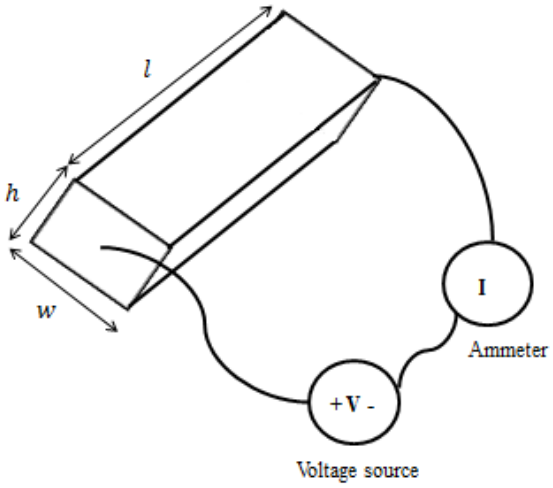

Figure 5. The schematic representation of the application of the two – point technique for electrical measurements.

A current I flows through the sample when applying a voltage V over it, induced by a voltage source. It is even possible to apply a current through the sample, inducing a voltage over it, measurable with a voltmeter in parallel with the current source. The ammeter shown in **Figure 5** is in series with the voltage source and the sample, and can be used to measure the amount of current passing through the rectangular bar, neglecting the voltage drop across the ammeter. By knowing the voltage level applied over the sample and measuring the current as explained above, Ohm's law may be used to evaluate the electrical resistance R as follows:

$$R = \frac{V}{I} \qquad \textbf{[10]}$$

where V and I are the voltage and the current as already mentioned, respectively measured in volt (V) and ampere (A), whereas the resistance R is measured in ohm (Ω).
This technique, even though easy and fast to apply, uses some approximations. Indeed, it neglects the resistances between the copper wires and the material, and even in the measuring equipment, responsible of an increasing resistivity. Even the nature of the contact between conductor wires and semiconductor sample could be considered as a problem concerning the surface currents. These issues could be solved using the four – point technique, not included in this report **[21]**.

2.8 Mechanical tests data elaboration: the Halpin – Tsai and the Nielsen models

In order to analyze the experimental data obtained by the mechanical tests performed on the nanocomposite of interest, two main models can be employed: the Halpin – Tsai and the Nielsen models. They can allow estimating the tensile modulus E_C, and this analysis can be connected to the electrical percolation evaluation, guaranteeing a more reliable report on the electrical and mechanical performances of the material. An important parameter such as the filler aspect ratio (length/diameter) has to be known before proceeding with the modeling, but its recognition is complicated in case of small sizes of the filler, as typical for GNP.

2.8.1 The Halpin – Tsai model

The Halpin – Tsai model permits a prediction of the tensile modulus of the composite system E_C as a combination of both the longitudinal tensile modulus E_L and the transverse one E_T. It requires several parameters such as the tensile moduli of the matrix E_M and of the filler E_f, in addition to the filler volume fraction V_f and the filler aspect ratio $\frac{L}{d}$ (length/diameter), hypothesizing that the filler has a cylindrical shape as a fiber. For this reason, the Halpin – Tsai estimation is usually used to predict the value of the tensile modulus of composites filled with carbon nanotubes (CNTs) or glass and carbon fibers, being their shape suitable to this model.

An explanation of the Halpin – Tsai equations and assumptions can be found in the review by **Halpin [22]**, and also recent studies have reported on its application to composite systems **[5, 23]**, even in combination with modified formulations **[24, 25]**.

The longitudinal E_L and transverse moduli E_T are shown below **[5]**:

$$\frac{E_L}{E_M} = \frac{1+2\left(\frac{L}{d}\right)\eta_L V_f}{1-\eta_L V_f} \qquad \textbf{[11]}$$

$$\frac{E_T}{E_M} = \frac{1+2\eta_T V_f}{1-\eta_T V_f} \qquad \textbf{[12]}$$

where the parameters η_L and η_T have the following expressions:

$$\eta_L = \frac{\left(\frac{E_f}{E_M}\right)-1}{\left(\frac{E_f}{E_M}\right)+2\left(\frac{L}{d}\right)} \qquad \textbf{[13]}$$

$$\eta_T = \frac{\left(\frac{E_f}{E_M}\right)-1}{\left(\frac{E_f}{E_M}\right)+2} \qquad \textbf{[14]}$$

where the physical explanation for the parameters used has already been made.

As aforementioned, the tensile modulus of the composite system E_C can be estimated as a combination of both longitudinal tensile modulus E_L and transverse one E_T, both for 2D and for 3D randomly oriented fibers, as follows:

$$E_C = \frac{3}{8}E_L + \frac{5}{8}E_T \qquad \textbf{[15]}$$

$$E_C = \frac{1}{5}E_L + \frac{4}{5}E_T \qquad \textbf{[16]}$$

where equation **15** is applicable to a 2D randomly oriented fiber – filled system, whilst equation **16** is for a 3D randomly oriented fiber – filled composite.

2.8.2 The Nielsen model

The Nielsen model predicts the tensile modulus of a composite system E_C using several parameters, such as the tensile moduli of the matrix E_M and of the filler E_f, in addition to the filler volume fraction V_f, the maximum filler packing fraction φ_m and the Einstein coefficient K_E, strictly dependent on the filler aspect ratio. This model is well employed for more types of loadings than the Halpin – Tsai theory **[22]**. The Einstein coefficient K_E depends upon the filler shape: for example, for spherical fillers such as carbon black, it has the value of 2.5. The Einstein coefficient K_E is $2\left(\frac{L}{d}\right)$ for carbon nanotubes (CNTs), with $\frac{L}{d}$ as the aspect ratio (length/diameter), whereas for graphite nanoplatelets an expression as the following one has been used:

$$K_E = 2.5\left(\frac{D}{t}\right)^{0.645} \qquad \textbf{[17]}$$

with $\frac{D}{t}$ as the aspect ratio (diameter/thickness of the platelet). The diameter of the graphite platelet is typically 3200 nm, whilst its thickness is 7 nm.

Using these geometrical parameters, the Einstein coefficient K_E becomes equal to 130. This parameter includes the dimensional requirements of the Nielsen model, even though the dependence on the geometry is not clearly shown in the main Nielsen expression.

Another parameter which has to be introduced is the maximum filler packing fraction φ_m. According to previous rheological studies, a value of 0.2 for carbon black CB and carbon nanotubes CNTs has been used, whereas the graphite nanoplatelets GNPs had a φ_m of 0.3 **[5]**.

The following expression can be employing for the Nielsen modeling of the tensile modulus of composite E_C:

$$\frac{E_C}{E_M} = \frac{1+ABV_f}{1+B\psi V_f} \quad \textbf{[18]}$$

$$A = K_E - 1 \quad \textbf{[19]}$$

$$B = \frac{\left(\frac{E_f}{E_M}\right)-1}{\left(\frac{E_f}{E_M}\right)+A} \quad \textbf{[20]}$$

$$\psi = 1 + \frac{1-\varphi_m}{{\varphi_m}^2} V_f \quad \textbf{[21]}$$

All the parameters included in these formulas have already been mentioned and physically explained **[5]**.

3. Materials

3.1 Polymer matrix

The polymer matrix used for fabricating the composites was an ethylene – butyl acrylate copolymer, also called EBA, containing 17 wt% (weight percent) of butyl acrylate and with a density of about 0.9 g/cm^3 (supplied by Borealis AB, a company whose venue is located in Sweden, and that focuses on providing plastic materials to the infrastructure, automotive and advanced packaging markets across Europe, the Middle East and Asia). When analyzing the results, an approximated density of 1 g/cm^3 has been employed.

3.2 Fillers

3.2.1 Low – structure carbon black (LS – CB)

A low – structure carbon black (LS – CB), an oil – pelleted black pigment with a density of 1.8 g/cm^3, according to the technical specifications supplied by the producer company Cabot Corporation, was used in this work.

3.2.2 Exfoliated graphite nanoplatelets (GNP)

The exfoliated graphite nanoplatelets (GNP) used were xGnP (XG Sciences, USA) grade M5. Grade M particles have an average thickness of approximately 6 nm and a typical surface area of 120 to 150 m^2/g. Grade M is available with average particle diameters of 5, 15 or 25 µm. Indeed, the features of grade M5 are a thickness of 6 – 8 nm, a diameter of 5 µm, a density of 2.2 g/cm^3 and a surface area of 120 – 150 m^2/g.
The technical data sheet reporting the typical and main electrical and mechanical properties of xGnP graphite nanoplatelets Grade M is shown in **Table 2**.

Table 2. Main electrical and mechanical properties of xGnP graphite nanoplatelets Grade M.

Property	Value (parallel to surface)	Value (perpendicular to surface)	Unit of measure
Density	2.2	2.2	g/cm^3
Carbon content	>99.5	>99.5	%
Tensile modulus	1000	not available	GPa
Tensile strength	5	not available	GPa
Electrical conductivity	10^7	10^2	S/m

4. Experimental procedure

4.1 Compounding

In order to guarantee the most effective mixing between the pure polymer matrix EBA (with the shape of millimetrical spherules), and the powder of the fillers used, graphite nanoplatelets GNP and low – structure carbon black LS – CB, a Brabender mixing machine, shown in **Figure 6**, provided with a mixing chamber with a volume of 50 cm^3 (**Figure 7**), was used.

Figure 6. The Brabender mixing machine.

As shown in **Figure 8**, a display, located on the front part of the machine, gives an idea about one important requirement for the compounding: the equilibrium with regard for the temperature between the front and the back parts of the mixer.
Before performing the mixing procedure, a heating time of the machine of almost 30 minutes is required, in order to reach the temperature level of 180 °C on both parts of the machine, to be kept constant during the compounding. The thermocouples used to measure the temperatures of the different parts of the machine were K, made of Chromel (Ni, Cr) – Alumel (Ni, Al).
The polymer matrix and the fillers (**Figure 9**) were first weighed using a digital scale, shown in **Figure 10** (Mettler Toledo Sartorius Mechatronics, L420S model number), characterized by a capacity of 420 g and a readability of 0.001 g. Then the material was inserted into the mixing chamber, once a rotational speed of the mixing heads of 5 rpm was fixed. The insertion of the fillers into the mixing chamber is an important step of the compounding process, and required to be slow, in order not to spread the filler out, modifying dramatically the composition of the final product as composite. This may influence its electrical and mechanical properties.
A protective mask has to be worn during the insertion of the graphite nanoplatelets GNP, because of their high volatility, and thus their easy inhalation.

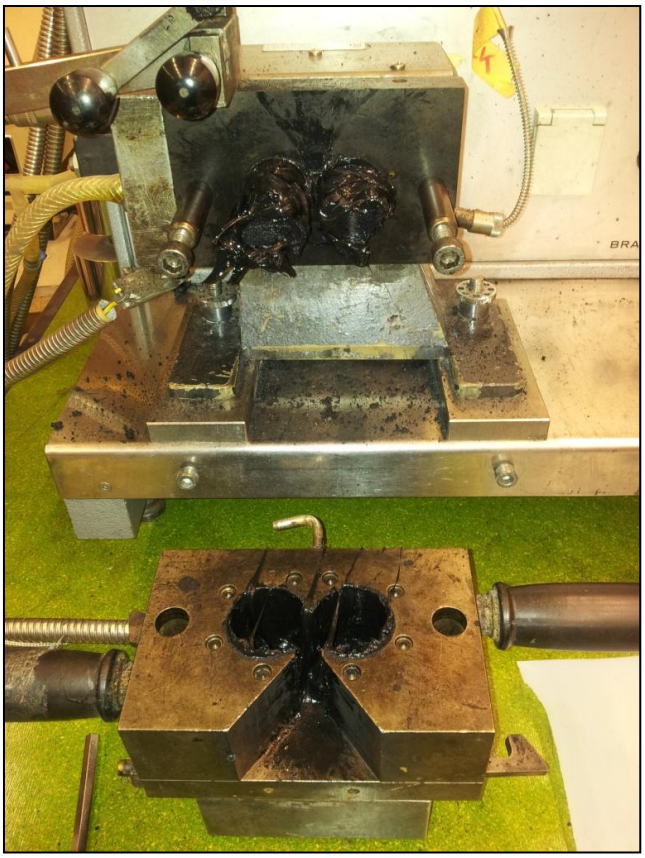

Figure 7. The details of the Brabender mixing chamber, with a volume of 50 cm^3.

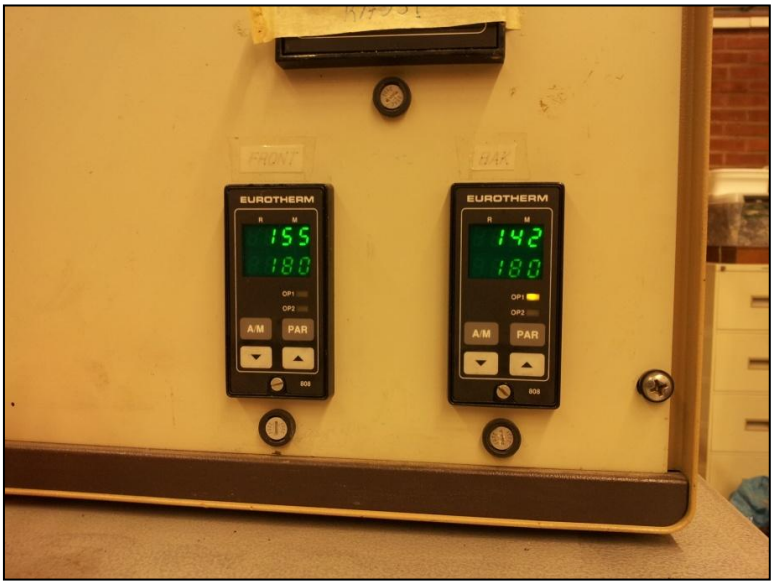

Figure 8. The display on the front part of the Brabender mixing machine, showing the temperature of the front and the back parts of the mixing chamber, on the left and on the right, respectively.

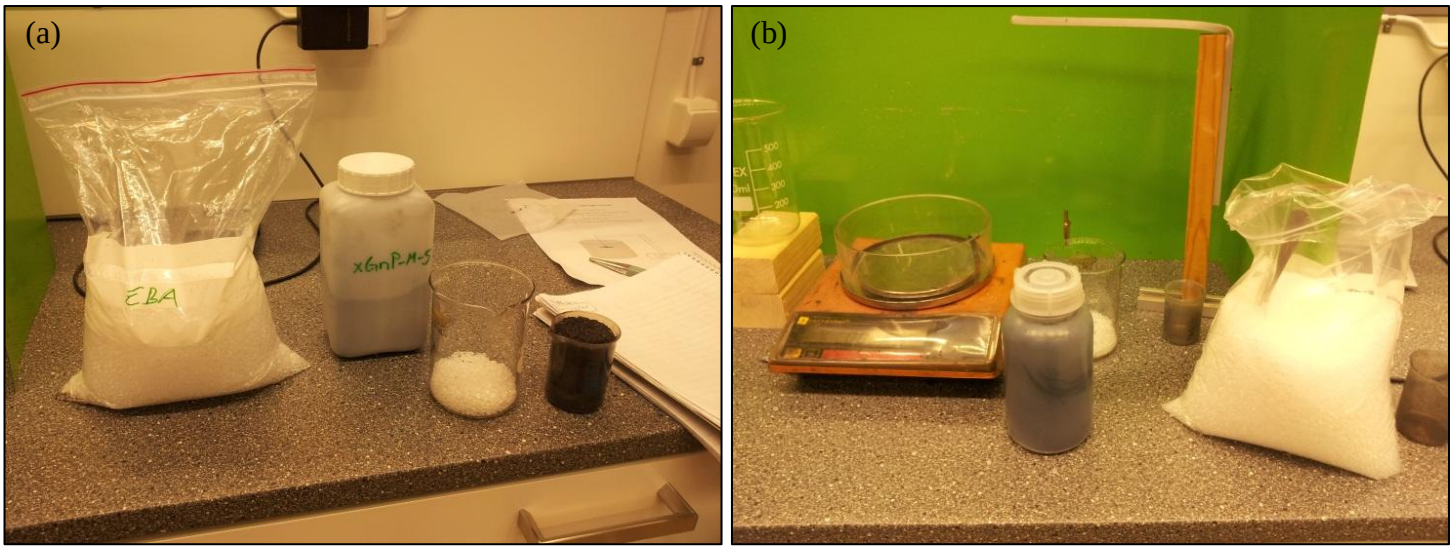

Figure 9. The polymer matrix EBA with (a) GNP (exfoliated graphite nanoplatelets) and (b) LS – CB (low – structure carbon black).

Figure 10. The digital scale (Mettler Toledo Sartorius Mechatronics, L420S model number), with a capacity of 420 g and a readability of 0.001 g, used to weigh the materials before the compounding process.

The mixing process was conducted with a rotational speed of the mixing heads of 100 rpm (revolutions per minute) for 10 minutes. The homogeneity of the compounding depends on the rotational speed, which should be constant during the mixing process: for this reason a handle, beside the display mentioned previously and located on the front part of the machine, allows a manual change of this parameter continuously.
After mixing the polymer matrix and the powder for 10 minutes, the following step was the removal of the final product (whose stickiness depends on the composition of the material), conducted with a rotational speed of the mixing heads of around 1 rpm.
The materials obtained with the mixing procedure were put on an aluminum or teflon foil, in order not to contaminate them from a contact with the work table. They were manufactured generating a series of composites of the pure fillers GNP and LS – CB, added to the pure polymer matrix EBA, and hybrids where the GNP was combined with LS – CB.
The hybrid compositions used for the tests (both electrical and rheological ones) were 80/20, 70/30 and 60/40, meaning the first number in the hybrid composition indicates the weight percentage of GNP of the total filler content, whereas the second number gives the weight percentage of the second filler employed, LS – CB.
The filler contents used for fabricating the composites tested were in the range of 0.9 – 15 vol% for the GNP systems, 3.1 – 16.3 vol% for the LS-CB materials and 2.9 – 16.8 vol% for its hybrids.
After each compounding process, a careful cleaning of the mixing chamber is required. This step has performed using a cleaning compound, known as Supernova. This odorless chemical process guarantees the removal of the residues from the mixing chamber.
It is essentially based on polyethylene, non – abrasive and does not damage aluminum, copper or steel. It is introduced, at the same temperature used previously (180 °C), into the mixing chamber before setting the same rotational speed of the mixing heads as employed for the previous mixing processes (100 rpm), but using a shorter time (around five minutes), in order to optimize the time of the fabrication procedure. The residue of the cleaning are then removed with the tools used for removing the final product after the mixing process. The cleaning process can ensure a lower contamination of the next material fabricated.

Another GNP/EBA system, with a composition of 8 vol% of GNP, was mixed in another Brabender mixing chamber, with a total volume of 300 cm^3, at 180 °C at 75 rpm for 4 minutes.
The aim of this last process was to produce materials for analyzing the influence of different steps of extrusion, and the resulting orientation given by this procedure to the material, on both electrical and mechanical properties, in particular Young's modulus (estimated in MPa) and the strain at break (%).

4.2 Extrusion step

The specimens being electrically and mechanically tested were fabricated from the extrusion of strings, using a capillary viscometer, Ceast Rheoscope 1000 6742/00 (Ceast SpA, Pianezza, Italy), shown in **Figure 11**. This machine has a capillary die made of hardened steel, and characterized by a length / diameter (*L/D*) ratio of 10/1 mm/mm.
Before introducing the material (reduced to small pieces to a size smaller than the piston) into the viscometer, a certain heating time to a temperature of 170 ^oC was needed, in order to ensure complete melting of the material. After homogenizing the pieces into the viscometer using a steel shaft, the strings were produced employing two piston speeds, 2 mm/min (equivalent to a shear rate of 24.3 s^{-1}) and a higher one, 20 mm/min (meaning a shear rate of 243 s^{-1}). The highest extrusion speed (20 mm/min) was used in order to produce a restricted set of samples (pure fillers/EBA system and a hybrid one, with a filler repartition of 80/20) for

evaluating the influence of the orientation of the anisometric fillers on the electrical and mechanical properties of the composites.
In a series of experiments the GNP/EBA system, with a composition of 8 vol% of GNP, mixed in a Brabender mixing chamber with a total volume of 300 cm^3, at 180 °C at 75 rpm for 4 minutes, was also subjected to an extrusion step. For this purpose a Brabender compact extruder, Brabender OHG (Duisburg, Germany), with a screw diameter *D* of 19 mm and a screw length of 25*D* (25 times the screw diameter), shown in **Figure 12**, was used. The screw used, shown in **Figure 13**, was a Maillefer barrier-flighted one (Maillefer, 1960; 1967) with a compression ratio 2.5:1 and with a Saxton distributive mixing element at the screw end. The temperature from the hopper to the circular die (with a diameter of 3 mm) was 150, 160, 170 and 180 °C. The screw speed used was of 100 rpm and the material was passed through the extruder three times, but some of the materials were collected after the first and second runs. The residence time in the extruder was approximately 1 minute.
After the three extrusion steps, the materials obtained were used to extrude specimens as strings at the different extrusion speeds (2 mm/min and 20 mm/min), employing the capillary viscometer (Ceast Rheoscope 1000 6742/00).

Figure 11. The capillary viscometer, Ceast Rheoscope 1000 6742/00 (Ceast SpA, Pianezza, Italy).

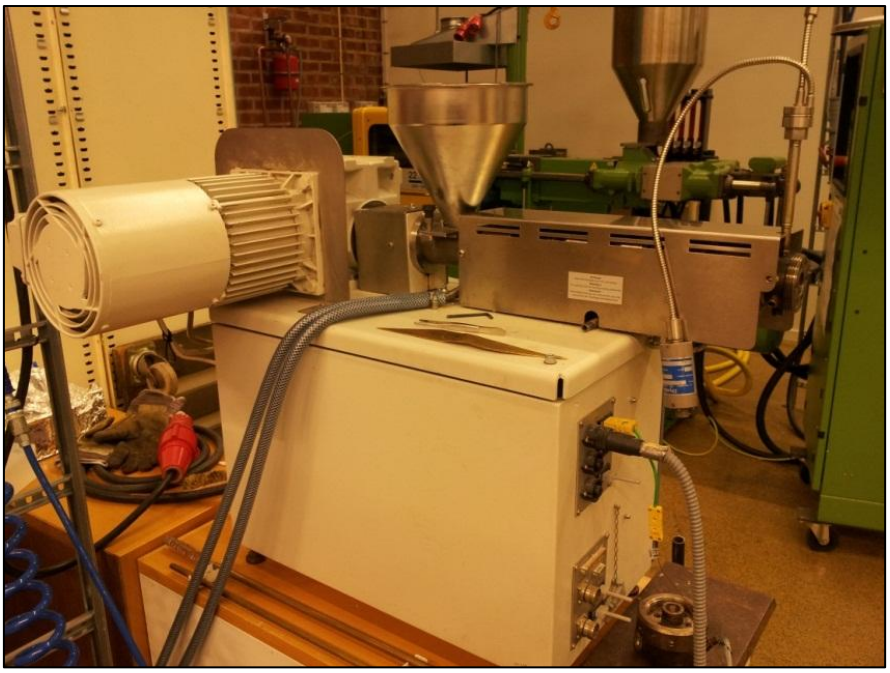

Figure 12. The Brabender compact extruder, Brabender OHG (Duisburg, Germany), with a screw diameter D of 19 mm and a screw length of $25D$ (25 times the screw diameter).

Figure 13. The Maillefer barrier-flighted screw (Maillefer, 1960; 1967) with a compression ratio 2.5:1 and with a Saxton distributive mixing element at the end.

4.3 Microstructural analysis

4.3.1 Sample preparation

The specimens were taken from the extruded strings from the capillary viscometer. Subsequently, they were ion polished perpendicularly to the flow direction, with a broad ion beam, Gatan Iliont model 693, USA, a machine typically employed for preparing planar cross sections from difficult samples for microscopic imaging and microanalysis. Its performance hinges on the proven Gatan PIPS™ (*Precision Ion Polishing System*), a robust platform with broad ion beam performance and reliability. The ion polishing was performed at 4 kV at -60 ^{o}C, in order to obtain a smooth surface of the sample for SEM observation.

4.3.2 Microstructural studies

Micrographs of the materials tested and analysed in the present work were obtained employing a JSM-7800F Thermal Field Emission Scanning Electron Microscope and a low vacuum JSM-6610 LV Scanning Electron Microscope, both from Jeol, Japan. The first SEM has an acceleration voltage of 3 kV, a hybrid objective lens with a resolution of 0.8 nm at 15 kV and 1.2 nm at 1 kV (it allows revealing extremely fine surface structures thanks to the very low incident electron energy), and the distribution of materials can be observed even at 0.5 kV. The second equipment enables observation of samples up to 200 mm in diameter, and the low vacuum mode can be chosen to analyze specimens not viewable at high vacuum because of excessive water content or a non-conductive surface. Another important feature is the acceleration voltage of 15 kV.

4.4 Electrical analysis

4.4.1 Sample preparation

The strings, taken manually with pincers from the capillary viscometer, were put between the two bars of a steel holder and reduced to a length, *l*, of 2.5 cm (as shown in **Figure 14**). Then the holder was put into a bowl containing liquid nitrogen (**Figure 15**), facilitating the fracturing process of the specimens, which were previously slightly incised using a small razor blade. The fracture surfaces of the specimens were then painted inside a fume box (shown in **Figure 16**) with conductive silver paint (previously shaken for a few minutes because of its sedimentation), occasionally diluted with iso – methyl – butyl – ketone (chemical formula $CH_3COCH_2CH(CH_3)_2$), as shown in **Figure 17**.

With this procedure, which avoids the increasing thickening of the paint in contact with the air, the diluent guarantees a good adhesion of the silver paint on both the fracture surfaces on the edges of the samples. In order to optimize the adhesion, a drying time, after the cryofracturing process in liquid nitrogen and the painting with silver paint, was needed for the samples, both painted and unpainted. These were then placed on supports into the fume box.

Both the painting and the occasional dilution of the paint were manually conducted with gloves into the fume box because of the issues regarding the irritability and toxicity of the silver paint and its diluent.

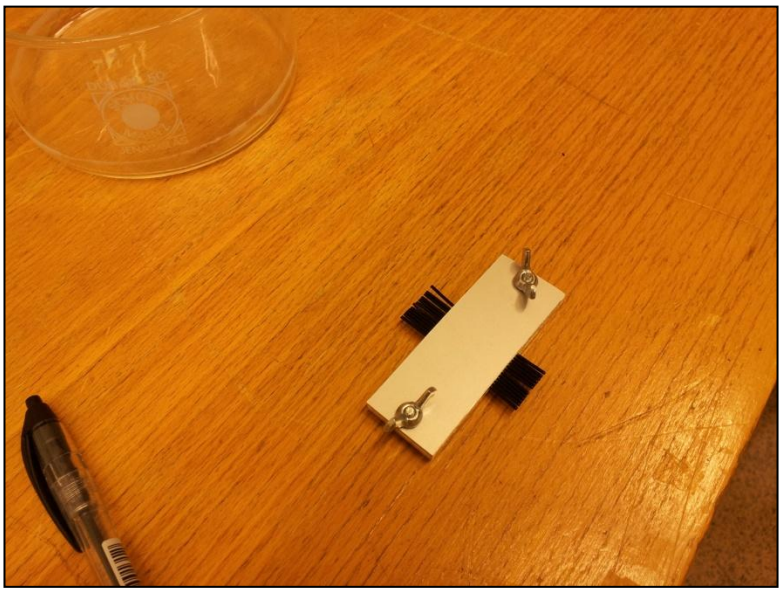

Figure 14. The steel holder used to put the specimens into the bowl with liquid nitrogen for the cryofracturing process.

Figure 15. The bowl with liquid nitrogen, for fracturing the composite specimens.

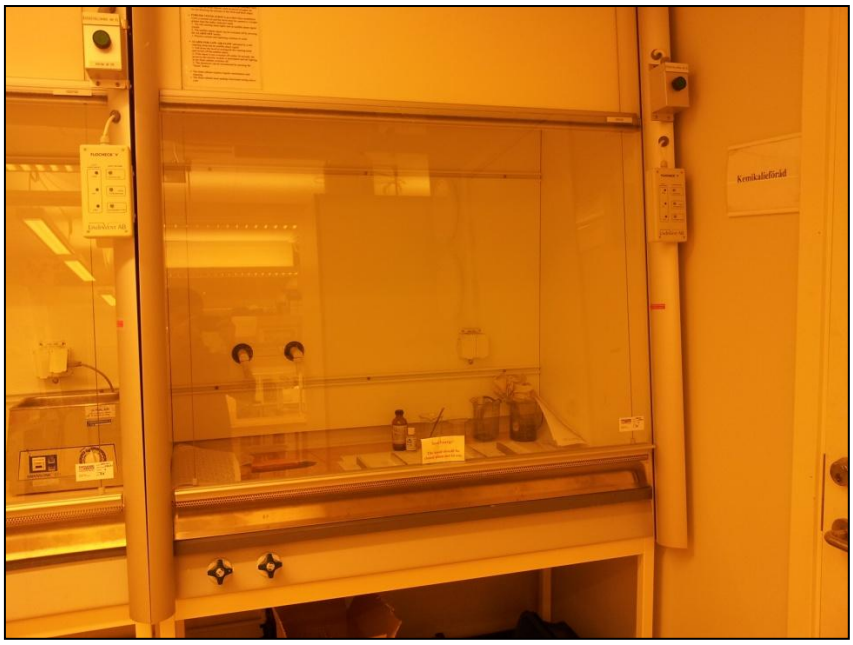

Figure 16. The fume box used for the processes of drying and painting of the specimens obtained after the cryofracturing step.

Figure 17. The conductive silver paint, on the right, and its diluent iso – methyl – butyl – ketone (chemical formula $CH_3COCH_2CH(CH_3)_2$), on the left.

4.4.2 Electrical tests

Electrical measurements were performed in order to assess the electrical conductivity of the samples obtained from the fabrication processes mentioned previously. The two-point technique was employed, according to *ASTM D257 - 07* standard test method **[26]**, also used in the work by **Spikowski *et al*. [21]** on CNT (carbon nanotubes) composites.
The samples, fabricated after the cryofracturing process of the extruded strings, were placed between two clamps as shown in **Figure 18**. Then they were subjected to the application of a voltage over their length.
In order to estimate the electrical resistance *R*, a Digital Multimeter Fluke 8846A (**Figure 19**) was employed.

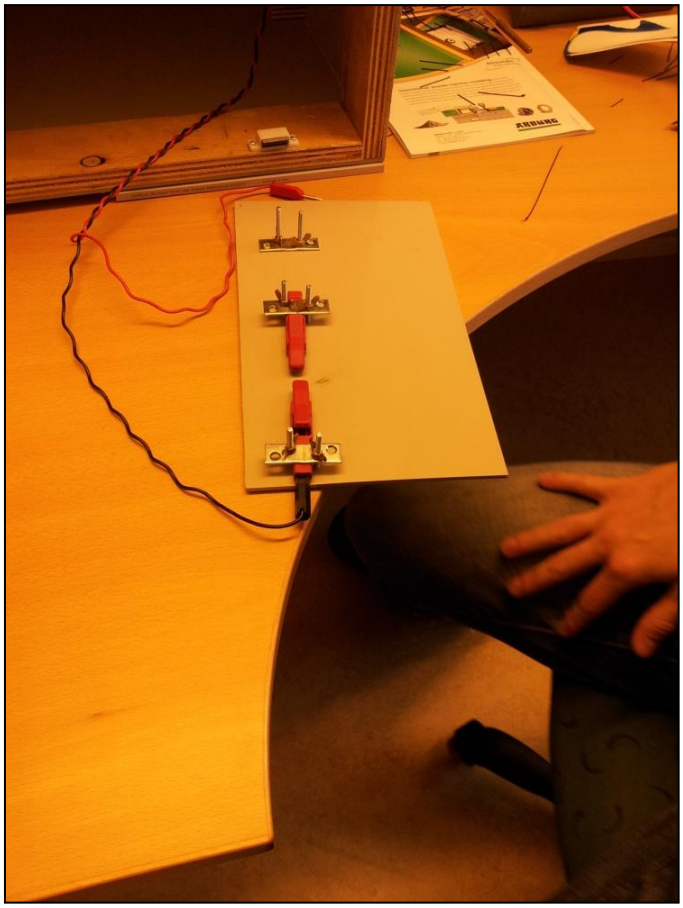

Figure 18. The clamps of the electrical test instrument, used to position the samples and to measure the electrical conductivity of the materials.

This instrument is equipped with a display for analyzing the experimental data in terms of real time plot or histogram, and this allows for recognizing possible signal quality problem. The electrical conductivity σ was determined as follows:

$$\sigma = \frac{l}{A \cdot R} \qquad [22]$$

where l represents the length of the samples (2.5 cm), A the cross section area (equal to $\frac{\pi \cdot D^2}{4}$, where D is the diameter of the single sample tested) and R, the electrical resistance of the material, measured by the multimeter.

Figure 19. The Digital Multimeter Fluke 8846A.

An electronic digital caliper, shown in **Figure 20**, was used to measure the diameter D of the samples. Its resolution is 0.01 mm, whereas it shows an accuracy of 0.03 mm.
Once located between the two clamps, the support equipment was inserted into the box for the electrical measurements **(Figure 21)**. Three different voltage levels were applied over the specimens: 10 V for composites with a conductivity higher than 10^{-3} S/cm, 100 V in case of conductivities between 10^{-5} and 10^{-3} S/cm and 300 V for conductivities lower than 10^{-5} S/cm.
As mentioned before, several systems (in terms of filler content and extrusion speed) were tested, and for each system 10 – 15 samples were used for the conductivity measurements.
The multimeter provides the maximum, the minimum and the average values of the current I flowing through the samples, even though the last one mentioned is the most useful in this case.

Figure 20. The electronic digital caliper used to measure the diameter D of the samples used for the conductivity measurements.

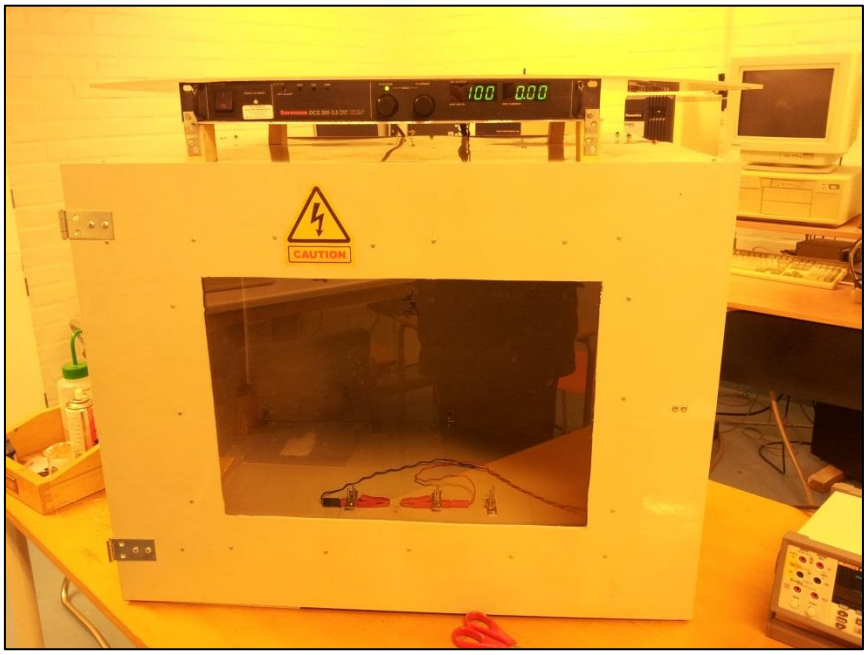

Figure 21. The box for electrical measurements where the support equipment for the samples is placed.

4.5 Rheological analysis

4.5.1 Sample preparation

The samples for rheological measurements were produced in the form of compression molded discs, with a diameter of 25 mm and a thickness of 2 mm, using a Bucher plastic press KHL 100 (typically employed for manufacturing plate – like semi – finished products using

thermoplastic plastics), shown in **Figure 22**. The samples were produced using a frame – like mold at the temperature of 180 ^{o}C with a cycle time of 10 minutes.

Figure 22. Bucher plastic press KHL 100.

4.5.2 Rheological measurements

A stress-controlled rotational rheometer, Rheometrics SR 200 was used at 180 ^{o}C under N_2 atmosphere for evaluating the viscoelastic properties of the materials. A parallel plate fixture was used, and all measurements started with a dynamic time sweep at 0.5 Hz, using a low stress until stabilization of the storage modulus G' had taken place. Several dynamic stress sweeps were then performed with the aim of valuating the threshold of the linear viscoelastic region. The dynamic frequency sweeps were conducted well below this threshold from 10 Hz down to 0.002 Hz. Each system was characterized by the average value of two or three measurements.

4.6 Mechanical properties

4.6.1 Sample preparation

The specimens being mechanically tested were the extruded long strings, from the capillary viscometer, Ceast Rheoscope 1000 6742/00 (Ceast SpA, Pianezza, Italy, **Figure 11**). The strings were obtained employing two different piston speeds, 2 mm/min (equivalent to a shear rate of 24.3 s^{-1}) and a higher one, 20 mm/min (meaning a shear rate of 243 s^{-1}), during the capillary extrusion. This choice, as explained previously, was made with the aim of evaluating the influence of the extrusion speed on the mechanical properties of the composites.

The time for the extrusion with the speed 2 mm/min was fixed to 20 minutes, in order to avoid the thermal degradation of the material extruded because due to a too long residence time inside the capillary.
A conveyor belt for CAN (*Controller Area Network*) connection (Brabender GmbH & Co. KG, model number 846102), shown in **Figure 23**, was placed next to the capillary hole, for taking off and transporting the extruded strings. Together with the speed control unit, the conveyor belt was mounted on a movable frame, adjustable in height. The wheels could be fixed. This type of conveyor belt permitted the nominal speed of the frame to be set by a personal computer software. The main features of the equipment are listed in **Table 3**.

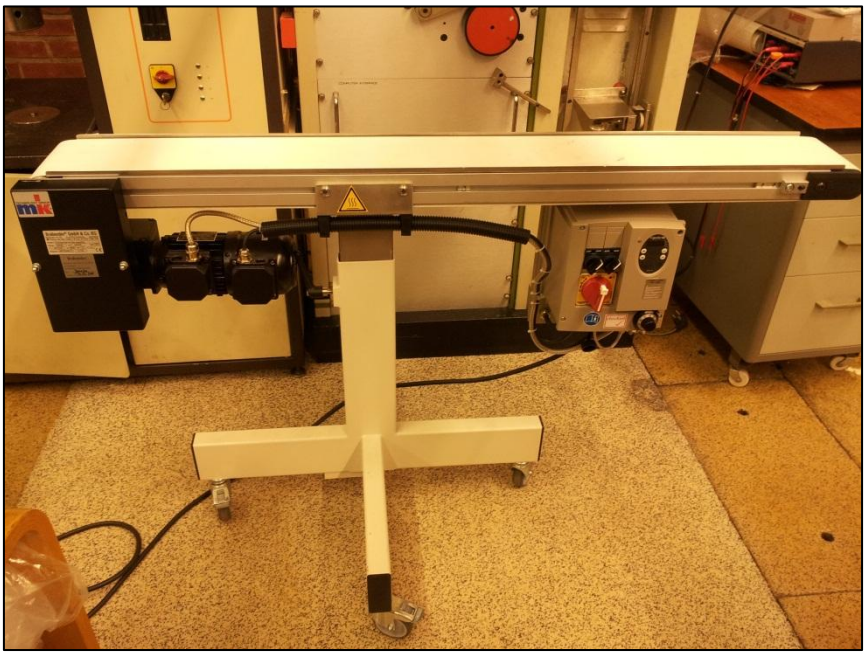

Figure 23. The conveyor belt for CAN (Controller Area Network) connection (Brabender GmbH & Co. KG, model number 846102).

Table 3. The main characteristics of the conveyor belt for CAN connection Brabender GmbH & Co. KG, model number 846102.

Parameter	Value
Speed	0.6 - 6.0 m/min (continuously adjustable)
Dimensions (width · initial height · length belt)	120 · 1150 · 1250 mm
Mains	230 V, 50 - 60 Hz, 0.4 A

During the experiments, the speed of the frame was fixed manually with a small knob, (shown in detail in **Figure 24**). The target was to find a perfect match between the extrusion speed of the strings from the capillary die and the speed of the conveyor belt, ensuring a homogeneous diameter of the final long string obtained. This is very important for estimating the mechanical properties of the material with a good reliability.

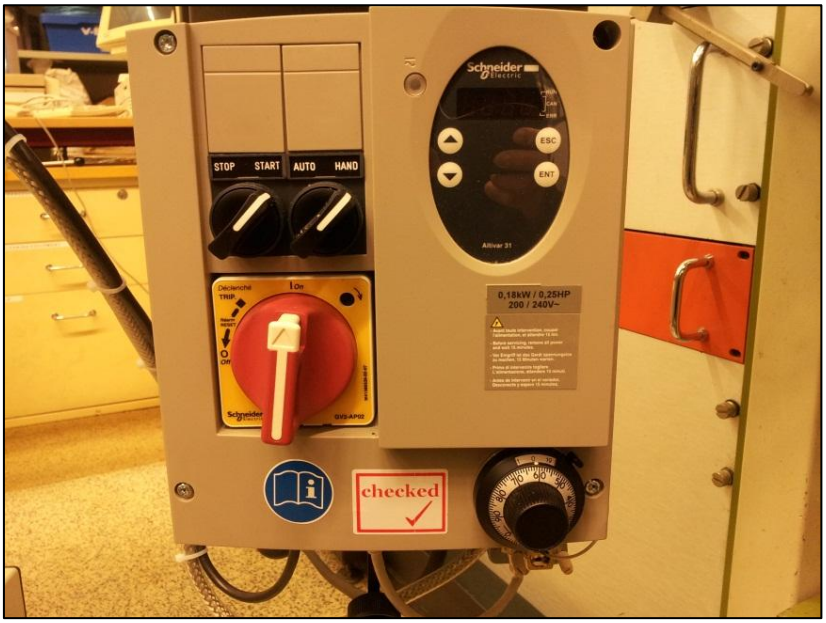

Figure 24. The detail of the knob (at the bottom on the right) for the manual control of the speed of the conveyor belt frame.

4.6.2 Mechanical tests

Uni axial tensile tests were performed on the strings of the EBA (ethyl butyl acrylate) composites, containing the different fillers in different amounts. Five specimens for each system and for each extrusion speed, 2 mm/min and 20 mm/min, all having a gauge length of 50 mm (the length of for the starting sample, as long extruded string, was 80 cm) were tested at room temperature. A hydraulic tensile tester for quasi – static tests, Zwick Z2.5 Tensile testing machine, equipped with a load cell of 500 N (manufactured by A. S. T. GmbH Dresden), was used. The filler contents of the systems were 1.9 – 15 vol% for the GNP systems, 3.1 – 16.3 vol% for the LS – CB materials and 2.9 – 15.3 vol% for one of the hybrids manufactured previously, with a filler repartition of 80/20, meaning the first number indicates the weight percentage of GNP of the total filler content, whereas the second number concerns the weight percentage of the second filler employed, LS – CB. This choice of hybrid system was motivated by the electrical tests results on the percolation thresholds and the electrical conductivity: this hybrid appeared to be the most interesting one.

The tensile tests were also performed on another GNP/EBA system, with a composition of 8 vol% of GNP, mixed in a Brabender mixing chamber, with a larger total volume (300 cm^3), maintaining 180 °C as constant temperature for 4 minutes. The rotational speed of the mixing heads was set to 75 rpm.

The strings being mechanically tested were extruded using a Brabender compact extruder, Brabender OHG (Duisburg, Germany), with a screw diameter D of 19 mm and a screw length of 25D (25 times the screw diameter). As mentioned before, the screw used was a Maillefer barrier-flighted one (Maillefer, 1960; 1967) with a compression ratio 2.5:1, and with a Saxton distributive mixing element at its end. The temperature profile from the hopper to the circular die (with a diameter of 3 mm) was 150, 160, 170 and 180 °C. The screw speed used was 100 rpm and the material was passed through the extruder three times, but some of the materials were collected after the first and second run. The residence time in the extruder was approximately 1 minute. The aim was to analyze the influence of different steps of extrusion on the mechanical properties, in particular on the tensile modulus (in MPa) and the strain at break (%). The first parameter was obtained as the slope of the linear part of the stress – strain curve for the samples tested. A strain range between 2 – 8 % of strain was conventionally chosen for all the specimens when determining the modulus, and each composition was represented by the mean value of five tensile tests.
As shown in **Figure 25**, the samples were mounted on a particular test configuration, with a compression preload not higher than 0.2 N, adjustable by checking the value on the personal computer display.

Before starting with the tensile tests, the parameters setting by the personal computer was mandatory, using a software named *testXpert V5.01*. The main process parameters to be set were the *test speed* and the *grip to grip separation*. The first parameter refers to the movement speed of the upper grip connected with the load cell mentioned before, whereas the lower grip is fixed to the basement. The test speed was set in order to obtain a strain rate of 100%/min. The *grip to grip separation* refers to the distance between the center of the round surface characterizing the grips. This parameter was set to 50 mm. Another useful parameter to be fixed before testing the materials was the upper and the lower limit of the grip run, which permits setting the *grip to grip separation* and to stop automatically the test at a certain level of load.

Figure 25. The tensile test configuration in the hydraulic tensile tester for quasi – static tests, Zwick Z2.5 Tensile testing machine, equipped with a load cell of 500 N (A. S. T. GmbH Dresden).

5. Results and discussion

5.1 Microstructural studies

Figure 26 and **27** show SEM images, of the surface of extruded specimens (*ion – polished*) of the 80/20 GNP/HS – CB (5.6 vol%) in EBA. In particular, **Figure 26**, taken at 2000x magnification, shows a well recognizable microstructural effect given by the extrusion process, meaning needlelike GNP structures parallel to the surface of the specimen and clearly oriented in the flow direction. It can be noticed how these structures tend to agglomerate, revealing a low effectiveness of the compounding step, and this reduces the surface area of the filler.

Figure 27, taken at higher magnification (20000x, even though the marker shown at the bottom of the micrograph is more reliable), gives an idea of the real configuration of the agglomerates, consisting of very thin platelets. This micrograph also shows the presence of apparently isolated platelets in the polymer matrix, thinner than 20 nm. The mentioned apparently isolated platelets and agglomerates were to some extent connected to each other due to a homogeneous dispersion of HS – CB particles.

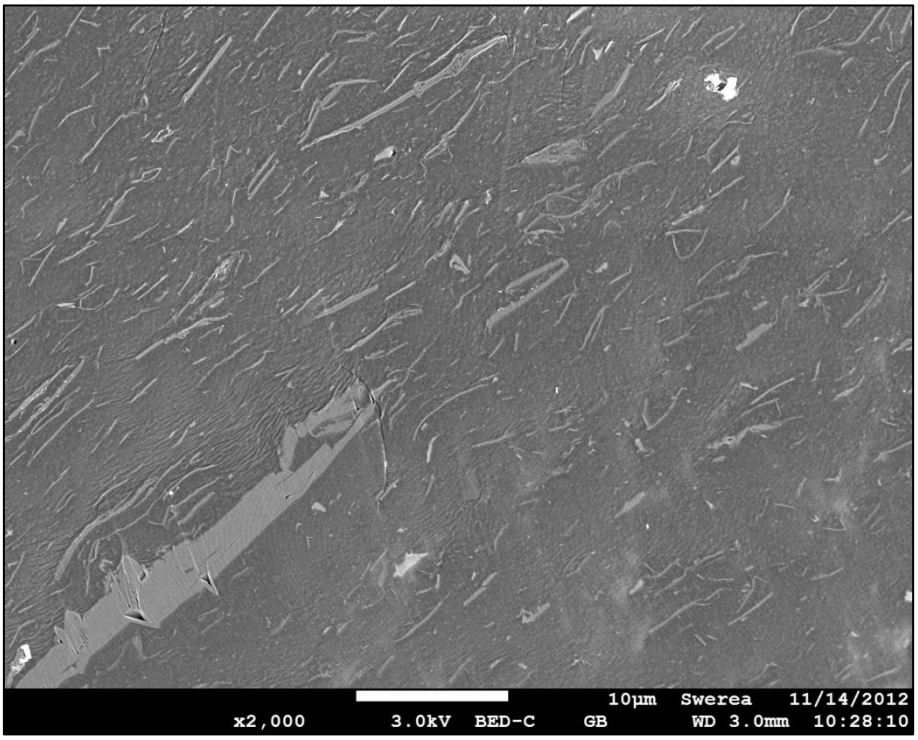

Figure 26. SEM micrograph of the 80/20 GNP/HS – CB (5.6 vol%) – EBA composite (2000x magnification).

Although the micrographs commented on above refer to one of the GNP/HS – CB – EBA composite system, the same effects may be identified in a composite filled with GNP/LS – CB. In particular, the orientation effect in the flow direction, given by the extrusion step, can be evidently found even in a pure GNP (9.1 vol%) in EBA system, as shown in **Figure 28**.

Nevertheless, the most important difference between the two systems shown was a more pronounced tendency towards aggregation of the GNP particles in the pure GNP/EBA system, compared to the situation in the hybrid composite.

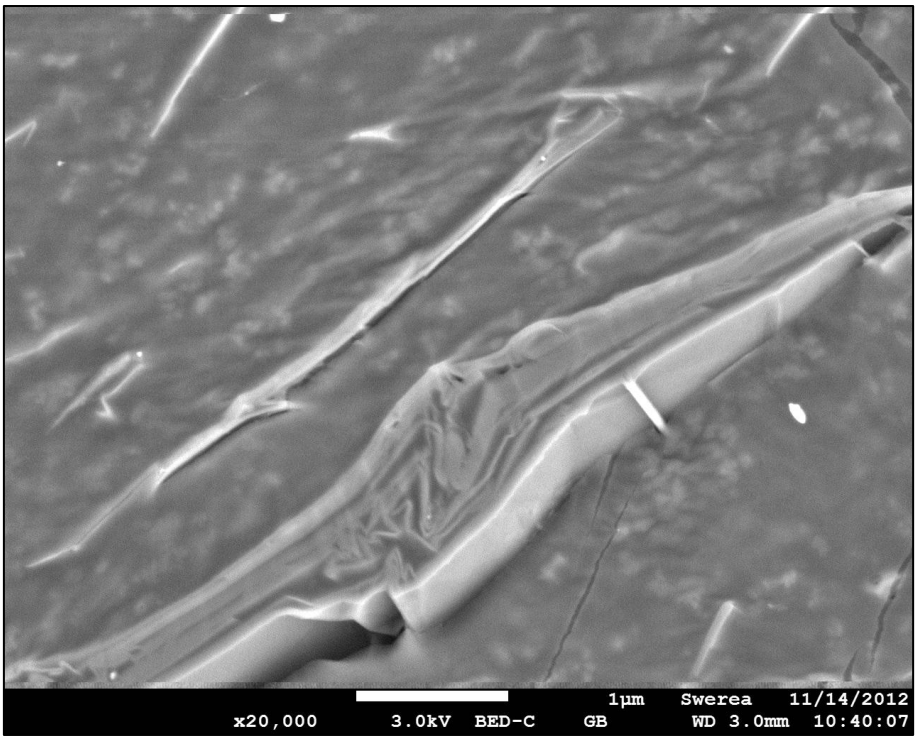

Figure 27. SEM micrograph of the 80/20 GNP/HS – CB (5.6 vol%) – EBA composite (20000x magnification).

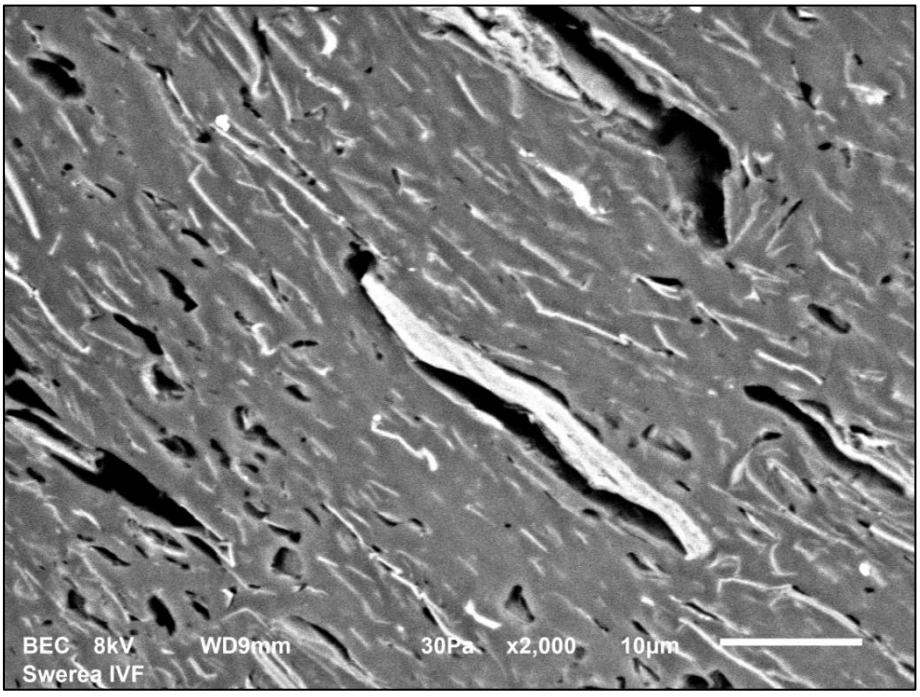

Figure 28. SEM micrograph of the pure GNP (9.1 vol%) – EBA composite (20000x magnification).

5.2 Electrical properties

A first observation from the results obtained from the electrical testing is evident from **Figure 29**, which shows the electrical conductivity (S/cm) as a function of the voltage (V) for the system with 8 vol% of GNP in EBA. The different points refer to repeated measurements on different samples of the same composition. This graph reveals an enhanced electrical conductivity with increasing applied voltage, a behavior explainable by the homogenizing effect of a higher voltage on the connections between the filler platelets. Another consideration that can be extracted from the graph, and explainable as for the first effect, was the diminution of the data scattering at higher voltages. These two results were found to be typical for most of the composite systems studied during the experimental work.

Figure 30 shows the electrical conductivity (S/cm), as a function of the filler volume content, for the systems made of ethyl butyl acrylate EBA filled with graphite nanoplatelets GNP, low – structure carbon black LS – CB and several hybrids containing both the fillers in different proportions between them, obtained with an extrusion speed of 2 mm/min.In particular 80/20, 70/30 and 60/40 (the first value is referred to the content of GNP, whereas the second value regards the content of LS – CB) were investigated. The most interesting results concern the percolation threshold and the electrical conductivity.

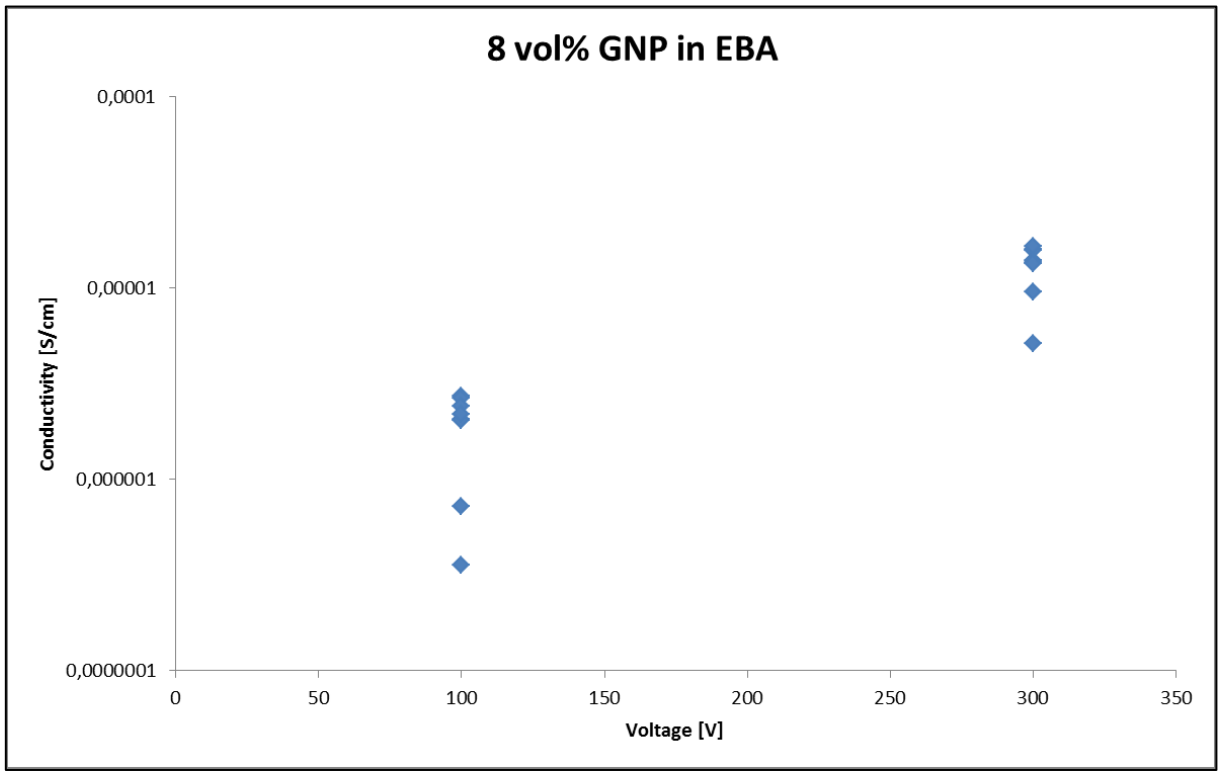

Figure 29. The electrical conductivity (S/cm) as a function of the voltage (V) applied over different specimens for the system 8 vol% of GNP in EBA.

The highest value of the percolation threshold belonged to the EBA/LS – CB system, equal to 11.7 vol% LS – CB. This value was much higher than the one noted for the EBA/GNP system (7.4 vol% GNP).

Although the EBA/LS – CB system had a higher percolation threshold than the EBA/GNP system, the addition of LS – CB to the latter system, developing a hybrid system, decreased the percolation threshold. The reason for this can be found taking into account the effectiveness of the LS – CB at creating a conductive network between the 2D – oriented GNP platelets: this so – called *synergistic effect* gave a considerable improvement in the electrical properties of the hybrid systems, resulting in a desirable decrease of the percolation threshold.
In the literature, a very interesting study about this effect can be found in the work by **Wei *et al*. [27]**. This report focused on the synergistic effect of combining graphite nanoplatelets GNP, spherical carbon black CB and long flexible carbon nanotubes CNTs, synthesized via a liquid mixing method with a different polymer matrix, epoxy resin. The main results of great interest were the effects on the percolation threshold and the higher conductivity of the nanocomposite with all the three fillers compared with the system filled with only one or two nanoparticles. A percolation threshold of 1 wt% and 0.5 wt% were found respectively for the systems with pure GNP and GNP/CB (*mass ratio* of 9:1), whereas the composite with all the fillers GNP/CB/CNT showed a value of only 0.2 wt% (*mass ratio* of 7:1:2). This result can be associated with the homogeneous dispersion of CB particles on the surfaces of GNP, in order to act as connection between the single graphite platelets, even though it could be thought that CB could prevent the agglomeration of GNP, causing a decrease in the number of the conductive paths. On the other hand, the reason for the enhanced electrical conductivity can to some extent certainly be associated with the small CB agglomerates filling the gaps between the GNP, and ensuring the formation of conductive links. In case of the presence of CNTs, the electrical conductivity can be optimized by bridging the graphite sheets, that can be well dispersed and therefore tough to connect each other.

Focusing again on the results of the present work, the *synergistic effect* was common to all the hybrid systems, except for the 60/40 system (meaning the 60 wt% of the filler content is GNP). Indeed, this system had a slightly higher percolation threshold compared to the one for the EBA/GNP system (7.7 vol% filler against 7.4 vol% GNP).
Another aspect is that a decrease of the LS – CB content in the hybrid systems gave a lower percolation threshold: the lowest values among the hybrids were noted for the 80/20 and 70/30 systems (with the 20 and 30 wt% of LS – CB of the total filler content, respectively), equal to 6.5 vol%, while 60/40 system had a percolation threshold of 7.7 vol%.
Despite the higher percolation threshold of the EBA/LS – CB system compared to EBA/GNP, the electrical conductivity of the former system was higher than the other at higher filler volume content (**Figure 30**).
A common trend was that for all the hybrid systems were more electrically conductive than the pure GNP system at higher filler loadings.
A summary of the electrical percolation thresholds obtained for the different composites is given in **Table 4**.

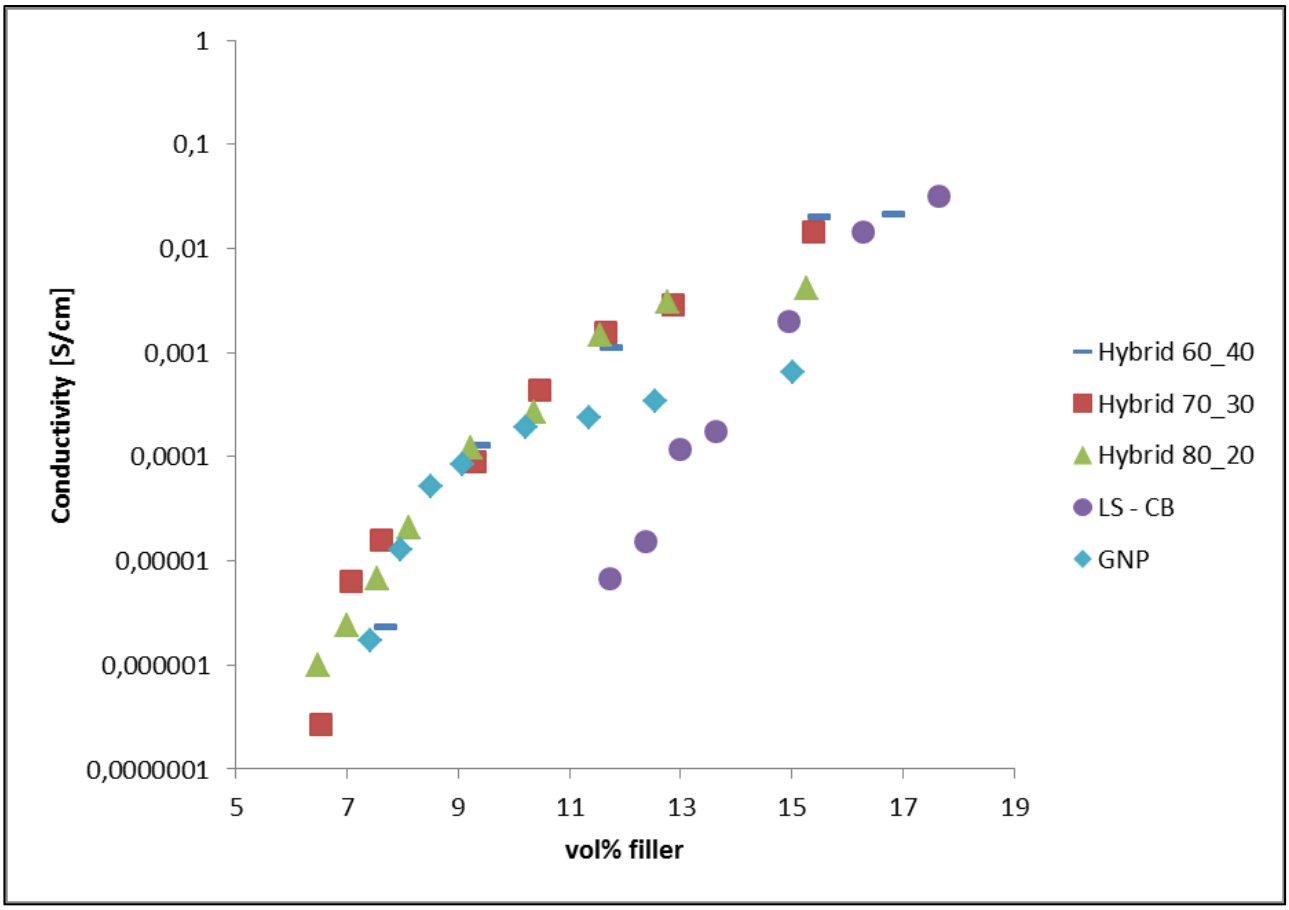

Figure 30. The electrical conductivity (S/cm) as a function of the filler volume content (vol%) for the different composites used in this work.

Table 4. The electrical percolation threshold (vol%) for the different systems.

System	Electrical percolation [vol%]
GNP	≈ 7,4
LS – CB	≈ 11,7
GNP/LS – CB 80/20	≈ 6,5
GNP/LS – CB 70/30	≈ 6,5
GNP/LS – CB 60/40	≈ 7,7

A comparison between nanocomposites containing low – structure carbon black LS – CB and high – structure carbon black HS – CB, in the same polymer matrix EBA could be made as shown in the work by **Oxfall [19]**. The electrical conductivity (S/cm) was studied as a function of the filler volume content (vol%) for a GNP/EBA system, containing different types of carbon black: LS – CB (same as in this work) or HS – CB. The high – structure carbon black was Ketjenblack EC 600JD (AKZO Nobel, Holland), with an aggregate size of 10 – 50 nm, density of 1.8 g/cm^3 and *BET* (*Brunauer, Emmet* and *Teller*) surface area of 1250 m^2/g, according to the producer. In **[19]**, the HS – CB system showed the lowest percolation threshold, around 2.1 vol% HS – CB (against 11.7 vol% LS – CB as the result of the present work), whereas the GNP exhibited the highest one, around 6.9 vol%.
The substantial difference in the percolation threshold between the two types of carbon black can be attributed to their difference in surface area (the *BET* area).
LS-CB was characterized by a much lower BET surface area than HS – CB, with the consequence of resulting in fewer conductive paths: this could give an explanation for the much higher percolation threshold of the LS – CB (in EBA). Nevertheless, both the LS – CB and HS – CB systems showed a much higher final conductivity at high filler volume content than the one with pure GNP.
Several studies can be found in literature concerning the influence on the electrical properties of introducing HS – CB into a non – conductive polymer matrix. A relevant example is given by **King *et al.* [28]**. In that work, a polycarbonate resin as polymer matrix and the same kind of HS – CB, Ketjenblack EC-600 JD, were used. A percolation threshold around 2.3 vol% HS – CB was found. Another interesting result was the decrease of the electrical resistivity by adding more HS – CB, from 1.3 10^{17} ohm · cm (for the neat polymer) to 20 ohm • cm for a composition of 10 wt% (6.9 vol%) HS – CB. HS – CB gave a lower electrical conductivity compared to a system with carbon nanotubes CNTs in the same polymer matrix, possibly due to the higher aspect ratio (length/diameter, equal to 1000) for CNT. The percolation threshold for the latter systems was between 0.7 and 1.4 vol% (1 to 2 wt%) CNT; the 8 wt% (5.6 vol%) CNT in PC (polycarbonate) composite showed a mean resistivity of 8 ohm · cm, lower than the one for HS – CB/PC composite **[29]**.

The influence on the electrical properties of the orientation of the anisometric fillers in the flow direction has been also investigated in the present work. For this reason, two different extrusion speeds, 2 mm/min and 20 mm/min, have been used, in order to obtain specimens with a different degree of filler orientation.
Figure 31 shows the electrical conductivity (measured in S/cm) as a function of the filler volume content for the EBA/GNP system. The composites were, as mentioned, extruded at two different speeds.

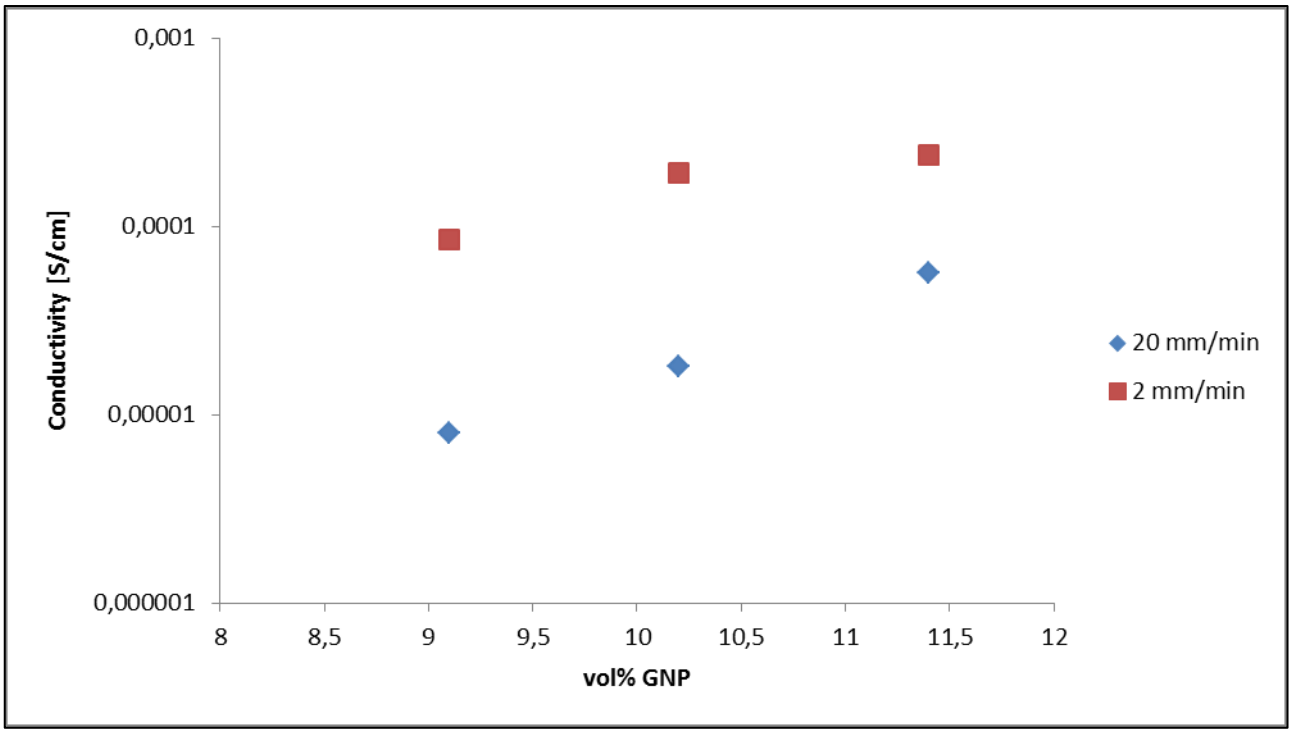

Figure 31. The electrical conductivity (S/cm) as a function of the filler volume of pure GNP in EBA, for specimens produced with two different extrusion speeds, 2 mm/min and 20 mm/min.

A remarkable result can be observed: the pronounced orientation of the graphite nanoplatelets, given by a higher extrusion speed, brought about a decrease of the electrical conductivity, even though the conductivity increased with an addition of more filler. The reason for this behavior can be attributed to a poorer particle – particle interaction. Furthermore, it can be noticed how the gap between the two trends decreased with increasing filler content, and this could possibly suggest a higher conductivity for the specimens obtained at 20 mm/min than the one at 2 mm/min, at higher volume fractions of GNP.
Another series of experiments was performed in order to assess the effect of several extrusion steps on the electrical properties of the nanocomposites filled with GNP. As explained above, this was made with the GNP/EBA system with 8 vol% of GNP, mixed in Brabender mixing chamber with a total volume of 300 cm^3, at 180°C for 4 minutes, setting the rotational speed of the mixing heads to 75 rpm.
A Brabender compact extruder, Brabender OHG (Duisburg, Germany), with a screw diameter D of 19 mm and a screw length of 25D (25 times the screw diameter), was used in order to obtain the specimens to be tested. The material was passed through the extruder three times at a screw speed of 100 rpm, but some of the materials were collected after the first and second run. The residence time in the extruder was around 1 minute. The results obtained are shown in **Figure 32**, which shows the electrical conductivity (measured in S/cm) as a function of the voltage (measured in V) applied across the specimens. Unlike the voltages of 100 V and 300 V used previously, voltage levels of 200 V and 300 V were taken as appropriate values, because of the negligible electrical conductivity of the composites at lower voltage levels.

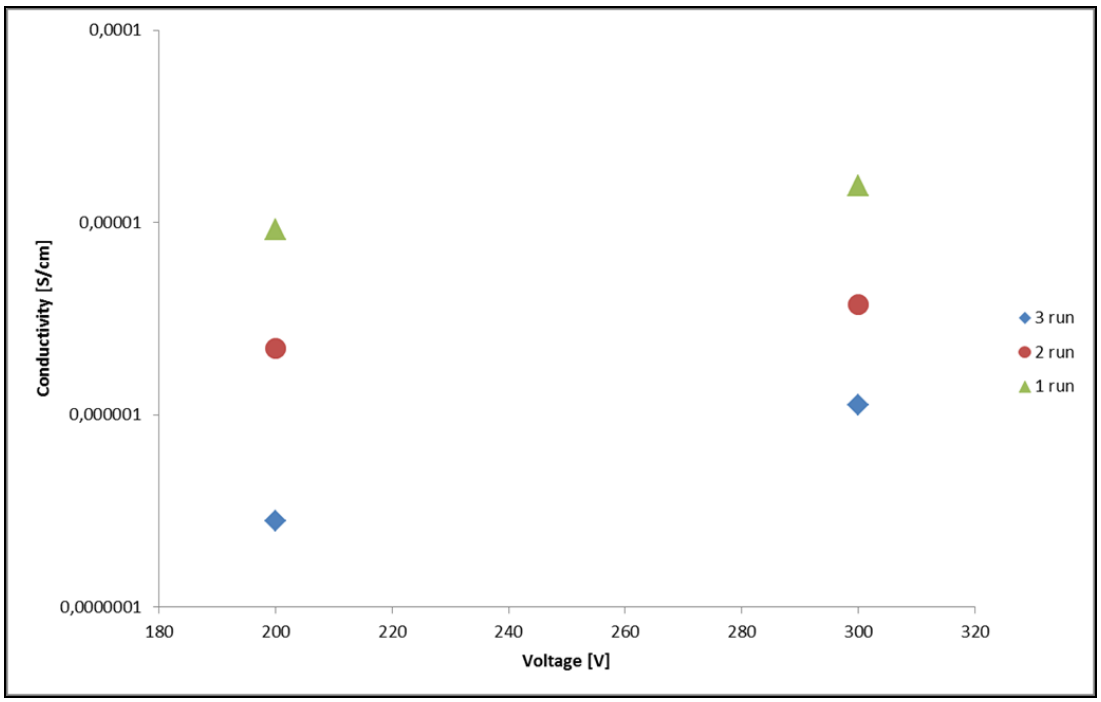

Figure 32. The electrical conductivity (S/cm) as a function of the voltage (V) applied over the specimens containing 8 vol% of GNP/EBA after three different extrusion steps.

The graph reveals a decreasing electrical conductivity, with an increasing number of extrusion steps. This result could appear to be in contrast with better homogeneity given by a more intense processing (increasing number of extrusion steps). The reason for this phenomenon can be suggested to be associated with a possible decrement of the conductive paths and interactions between GNP particles due to the mechanical stress imposed on the materials.
An increased applied voltage had as consequence an enhanced electrical conductivity and a decrease of the experimental scatter, as reported above for the other nanocomposite systems.

5.3 Rheological properties

As described previously, a stress – controlled rotational rheometer, Rheometrics SR 200 was used at 180 ^{o}C under N_2 atmosphere for evaluating the viscoelastic properties of the samples produced as compression molded discs, with a diameter of 25 mm and a thickness of 2 mm, in a Bucher plastic press KHL 100, using a frame – like mold at the temperature of 180 ^{o}C for a processing time of 10 minutes.

Figures 33, **34** and **35** show the storage modulus, G'(Pa) as a function of the frequency (Hz) for three of the systems containing GNP, low – structure carbon black LS – CB and the 80/20 GNP/LS – CB in EBA hybrid system (GNP is present with 80 wt% of the total filler content).
A first result can be identified in the flattening out of the storage modulus G' at the lower frequencies, showing a solid – like response. This trend can sometimes be correlated to the onset of the electrical conductivity.
It is possible to analyze the rheological performance of the materials tested with another method consisting in determining the filler content at which a *cross – over* of the storage modulus G' and the loss modulus G'' occurs at low frequencies. Indeed, at low filler loadings,

the loss modulus G'' is higher than the storage modulus G', meaning that the viscoelastic behavior of the composite mainly is governed by the viscous polymer matrix. This situation changes at increasing filler contents. At a certain filler content G' will exceed G'', a filler network is formed indicating a rheological percolation threshold **[20]**. Some values of rheological percolation are provided by **Table 5**.
An exact correlation between the electrical and the rheological percolations cannot be found: this is mainly due to possible crystallization phenomena and the totally different degree of order in the systems. Indeed, in this work, the specimens tested electrically were obtained after extrusion, which gave a particular orientation to the filler particles, whereas the specimens used for rheological analysis were unoriented. The explanation given does not exclude that there are some similarities between the two types of percolation limits (**Tables 4** and **5**).
Table 5 shows that the rheological percolation for the LS – CB/EBA composite is quite similar to the one found for GNP/EBA system (7.4 vol% and 8 vol% respectively). The effect of adding LS – CB to the GNP/EBA system caused a slight increase of the onset of rheological percolation (higher than 8 vol%).

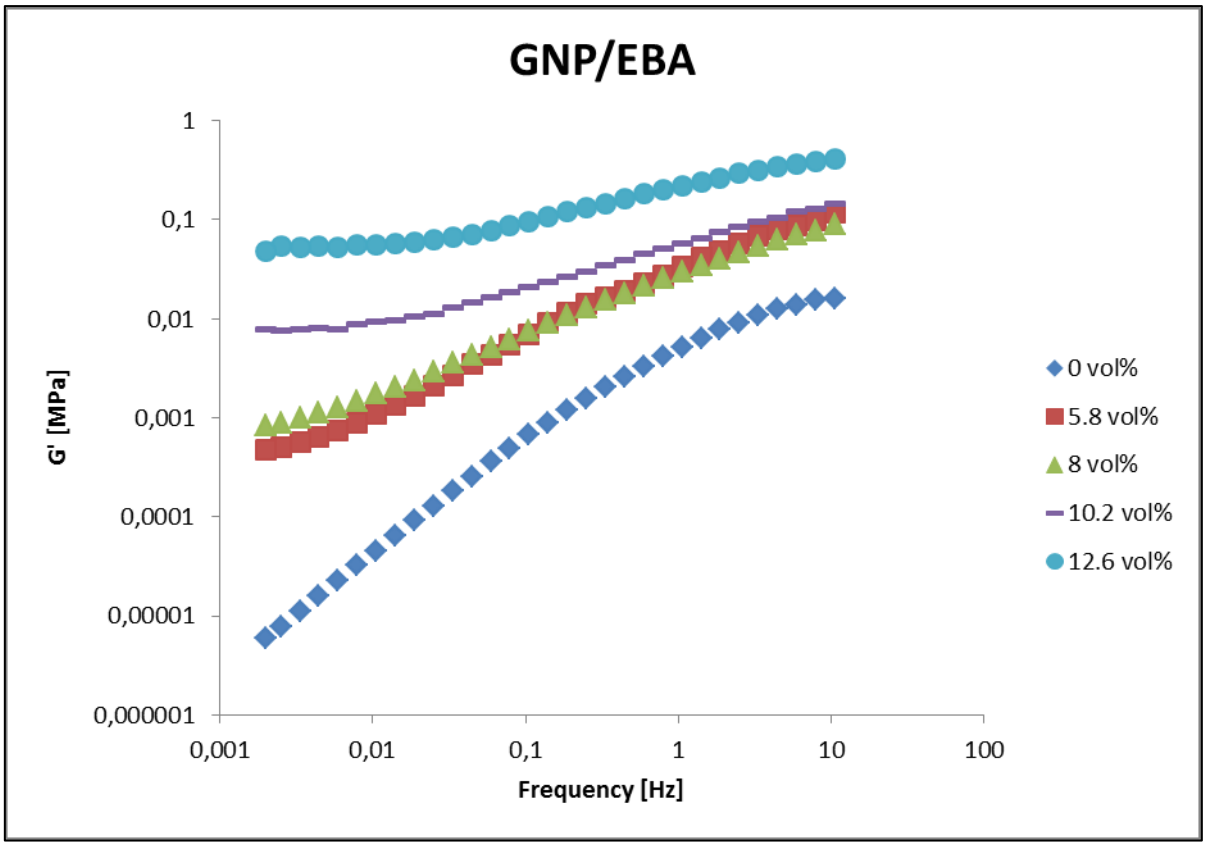

Figure 33. The storage modulus G' (MPa) as a function of the frequency (Hz) for the GNP/EBA composite at different filler volume fractions.

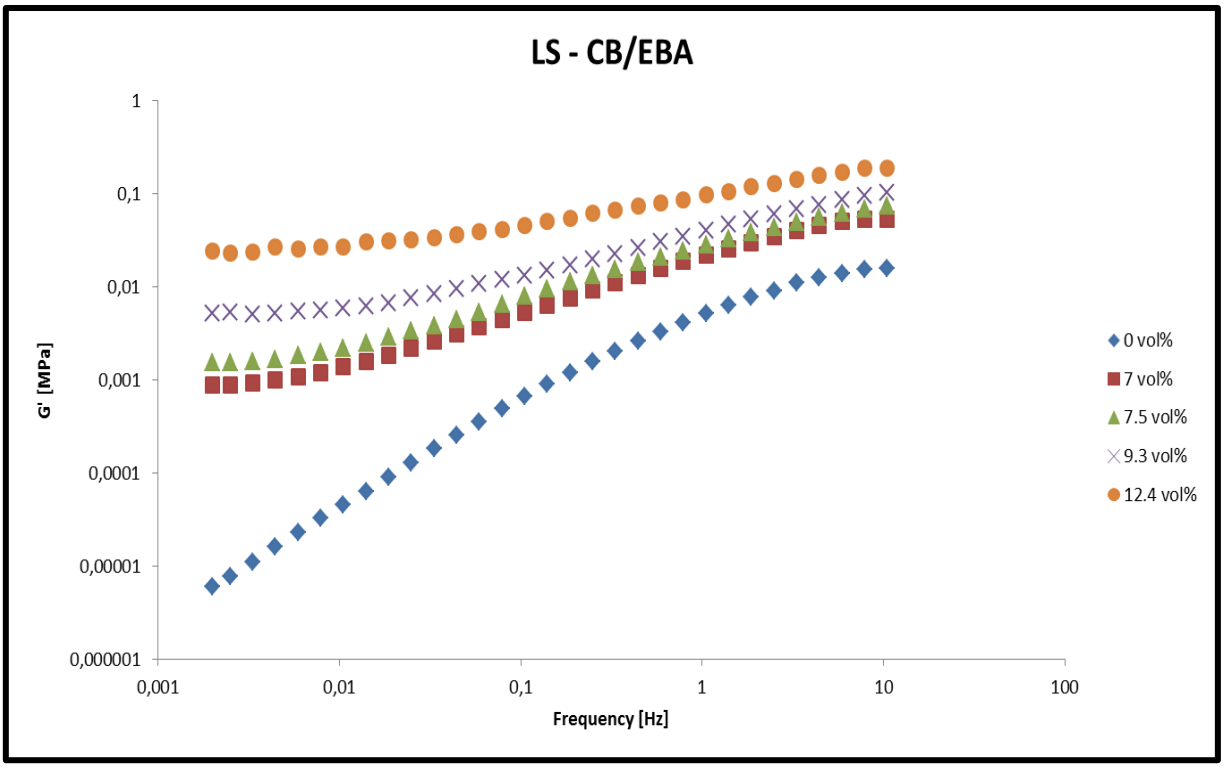

Figure 34. The storage modulus *G'* (MPa) as a function of the frequency (Hz) for the LS – CB/EBA composite at different filler volume fractions.

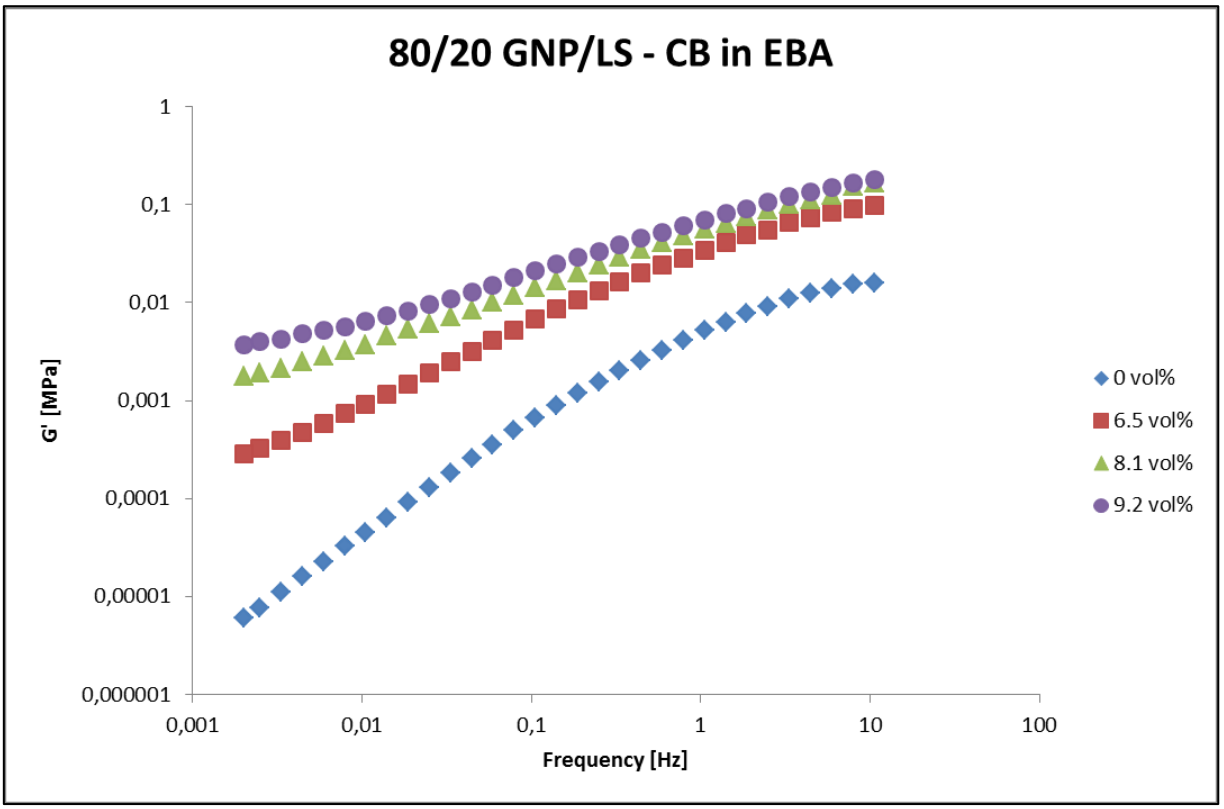

Figure 35. The storage modulus *G'* (MPa) as a function of the frequency (Hz) for the 80/20 GNP/LS – CB in EBA hybrid system at different filler volume fractions.

Analyzing again the correlation between the rheological and the electrical percolations, only a weak correspondence for the LS – CB/EBA systems was found. Indeed, the flattening out of *G'* at lower frequencies shown in **Figure 34** for the system just mentioned began at 7 vol% (with a rheological percolation threshold of 7.4 vol%), whereas the onset of the electrical conductivity amounted to a value within the range 11.4 – 12 vol%.
Regarding the hybrid containing LS – CB, the rheological percolation threshold was higher than the electrical one.

Table 5. The rheological percolation values (vol%) associated to the cross – over between *G'* and *G''*.

System	Rheological percolation [vol%]
GNP	8
LS – CB	7.4
GNP/LS – CB, 80/20	8.1

In order to make this study on the rheology of the produced composites more complete, a brief parallelism between the rheological and electrical percolation thresholds could be of interest. In **Figure 33**, related to the GNP/EBA system, the solid – like behavior of the composites was manifested at higher filler volume fractions, connected to the flattening out of the storage modulus *G'* at low frequencies. This behavior can be physically explained by the generation of a network of the platelets, which can ensure a mechanical reinforcement to the material. It can be also noted that the rheological percolation, of 8 vol% shown in **Table 5**, was slightly higher than the electrical one, reported in **Table 4**, of 7.4 vol%. The plateau behavior of the storage modulus *G'* at lower frequencies was manifested between 8 vol% and 8.5 vol%, very close to the cross – over between the moduli. From **Figure 34**, related to the LS – CB/EBA system, instead, it is clear the flattening out of *G'* was in the range 7 – 7.5 vol% and, by comparison with **Table 5**, this range can be considered reliable since the rheological percolation had a value of 7.4 vol%. The value of the rheological percolation for the hybrid system studied, equal to 8.1 vol%, reflects very well the flattening out of the storage modulus, noticeable in **Figure 35**.

The mismatch between the electrical and rheological percolation thresholds has been also reported by **Zheng *et al.* [30]**, who based their studies on a composite with HDPE (high density polyethylene) as polymer matrix and LS – CB as loading. The flattening out of the storage modulus *G'* at lower frequencies was shown to be around 15 vol%, whereas the electrical percolation threshold was around 9.5 vol%. It is important to remark that the

samples being tested electrically were disks about 1.5 mm thick, 100 mm wide, and 100 mm long prepared by compression molding (at 165 °C under 10 MPa) and cut into appropriate pieces, without giving any orientation due to an extrusion processing step. The reason for the poor correspondence between electrical and rheological percolations can be hypothesized as related to a possible crystallization behavior.

Oxfall [19] analyzed the electrical and rheological properties of both LS – CB and HS – CB composite systems. A comparison between the behaviors given by the two different types of filler can be worthwhile.

For the HS – CB system, it was noticed that the rheological percolation was lower than the electrical percolation threshold (**Tables 6** and **7**). The flattening out of G' was manifested at a value of 1.6 vol%, in fair agreement with the rheological percolation of 1.5 vol%, reported on **Table 7**. An addition of HS – CB to the GNP/EBA system lowered the rheological threshold below the electrical threshold in case of the 70/30 hybrid. Nevertheless, the main relevant result for the HS – CB systems was the good correspondence between the rheological and electrical thresholds, even though also in this case the orientation of the extruded specimens tested electrically could play an important role, influencing this correlation. The same behavior was found in PP (polypropylene) and PE (polyethylene) systems containing HS – CB by **Stråat *et al*. [31].**

Table 6. The electrical percolation threshold (vol%) for the systems containing HS – CB **[19]**.

System	Electrical percolation [vol%]
GNP	$6.4 < \omega_c < 6.9$
HS – CB	$1.8 < \omega_c < 2.1$
GNP/HS – CB, 90/10	$4.0 < \omega_c < 4.6$
GNP/HS – CB, 80/20	$3.7 < \omega_c < 4.2$
GNP/HS – CB, 70/30	$3.3 < \omega_c < 3.8$

Table 7. The rheological percolation values (vol%) associated with the cross – over between G' and G'' **[19]**.

System	Rheological percolation [vol%]
GNP	7.4
HS – CB	1.5
GNP/HS – CB, 90/10	5.2
GNP/HS – CB, 80/20	3.8
GNP/HS – CB, 70/30	3.2

5.4 Mechanical properties

As mentioned earlier, uniaxial tensile tests were performed on strings of EBA with addition of graphite nanoplatelets GNP, of low – structure carbon black LS – CB, and their hybrids. Five specimens for each system and for each extrusion speed, 2 mm/min and 20 mm/min, all having a gauge length of 50 mm (the length of for the starting sample, as long extruded string, was 80 cm), were tested. The filler contents were 1.9 – 15 vol% for the GNP systems, 3.1 – 16.3 vol% for the LS – CB materials and 2.9 – 15.3 vol% for one of the hybrids, with a filler repartition of 80/20 (80 wt% of GNP of the total filler content). The tensile tests were performed also for another GNP – EBA system, with 8 vol% of GNP, with the strings extruded using a Brabender compact extruder, Brabender OHG (Duisburg, Germany), with a barrier – flighted screw (**Figure 13**), diameter D 19 mm and a screw length of $25D$. The aim was to assess the influence of several extrusion steps on the mechanical properties, in particular on the tensile modulus (in MPa) and the strain at break (%). A range between 2 – 8 % of strain was conventionally chosen for all the specimens when evaluating the modulus, and each composition was represented by the mean value of five tensile tests.

In **Figure 36** and **37** the tensile moduli of the composite (MPa) and the strain at break (%) respectively, are shown as functions of the filler volume fraction (vol%) for the pure GNP/EBA system.

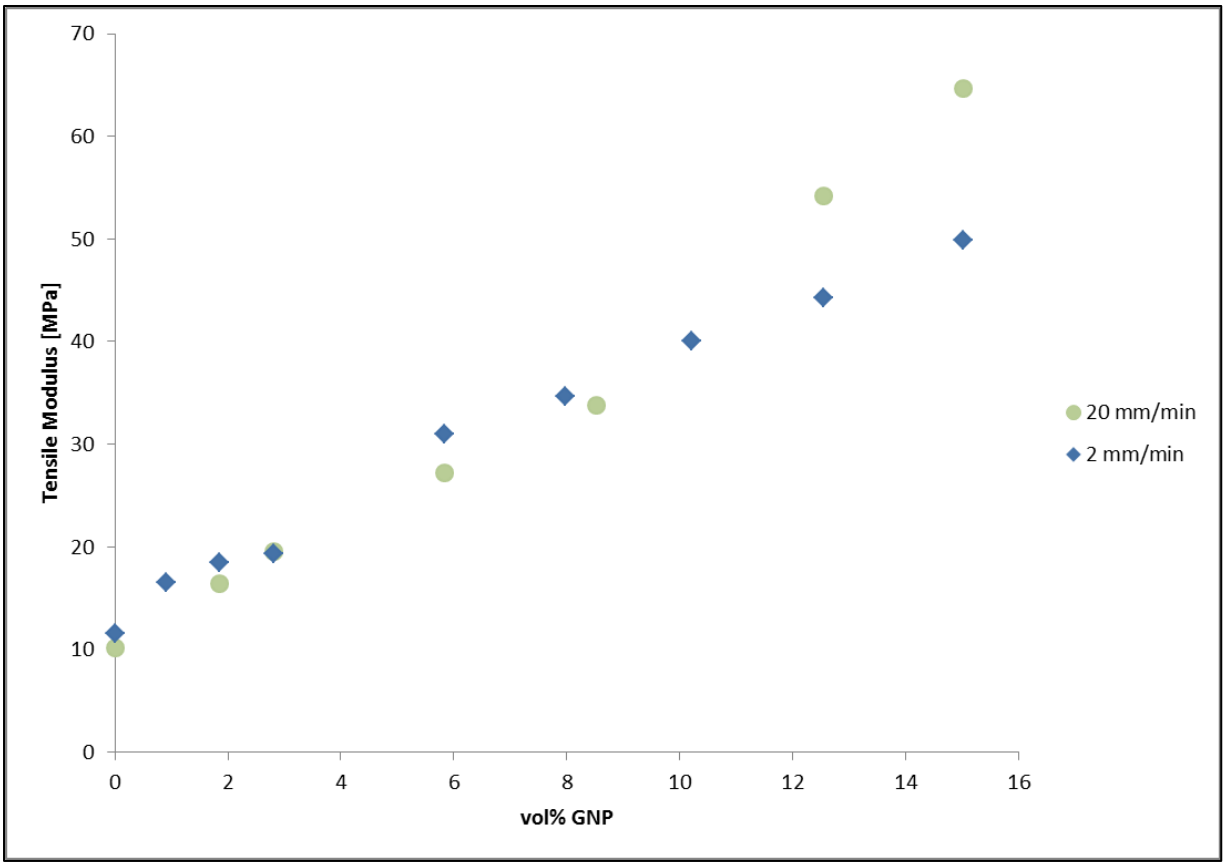

Figure 36. The tensile modulus (MPa) of the pure GNP/EBA system as a function of the filler volume fraction (%), related to two different extrusion speeds, 2 mm/min and 20 mm/min.

Regarding the tensile modulus, it can be noted from **Figure 36** that an addition of a small amount of GNP to the polymer matrix (0.9 vol%) gives an increase by 43.23%. **Kim *et al.* [2]** obtained similar results (increase by 55% of the tensile modulus by addition of 0.85 vol% of GNP), even though that work employed another polymer matrix, linear low density polyethylene LLDPE.

By comparing the behaviors related to the different extrusion speeds, the tensile modulus of the specimens produced at 20 mm/min, characterized by a higher degree of orientation of the agglomerates and platelets was about the same as for extrudates produced at 2 mm/mmin, at least up to a filler content of about 10 vol% of GNP. At higher filler contents, the modulus of the specimens extruded at the higher speed was the highest which probably can be associated with the more pronounced degree of orientation. Thus it may be argued that the influence of the orientation only becomes apparent at not for low filler contents.

Figure 37 shows that the strain at break decreased strongly with increasing GNP volume fractions, from around 350 – 550% at 2.8 vol% to around 30% for the highest filler volume content, 15 vol%. The strain at break was higher for the specimens produced at 20 mm/min for all of the compositions tested. This can be significant of a less brittle material as effect of the orientation.

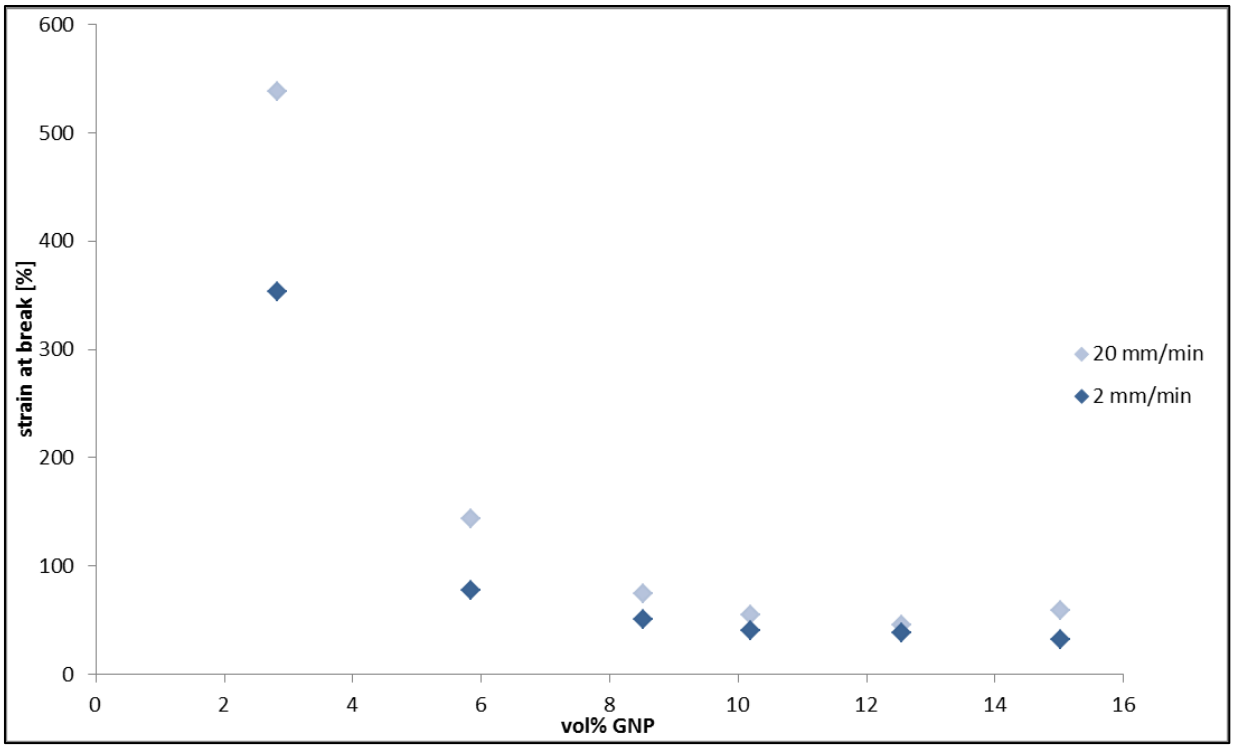

Figure 37. The strain at break (%) of the pure GNP/EBA system as a function of the filler volume fraction (%), related to two different extrusion speeds, 2 mm/min and 20 mm/min.

The pure polymer matrix did in this case not rupture: the tests were stopped automatically before it was attained, the EBA surely had at a strain at break of more than 1000%.

In **Figures 38** and **39** the tensile modulus and the strain at break, respectively, are shown as functions of the filler volume fraction, for the GNP/LS – CB in EBA hybrid system.

As shown in **Figure 38** the tensile modulus of the samples extruded at 2 mm/min was higher than those extruded at 20 mm/min, especially at higher filler contents. This is in contrast with the expected result and could perhaps be associated with a less homogeneous dispersion of the filler particles.

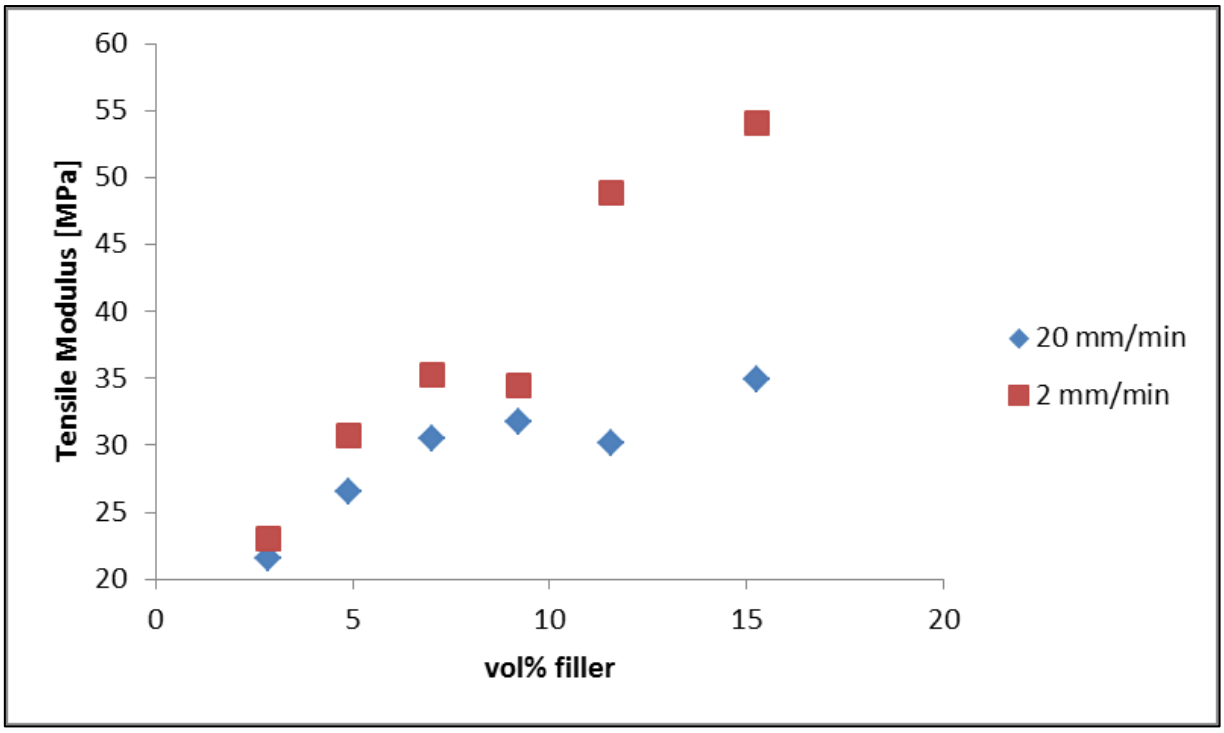

Figure 38. The tensile modulus (MPa) of the 80/20 GNP/LS – CB – EBA hybrid system as a function of the filler volume fraction (%), for the two different extrusion speeds, 2 mm/min and 20 mm/min.

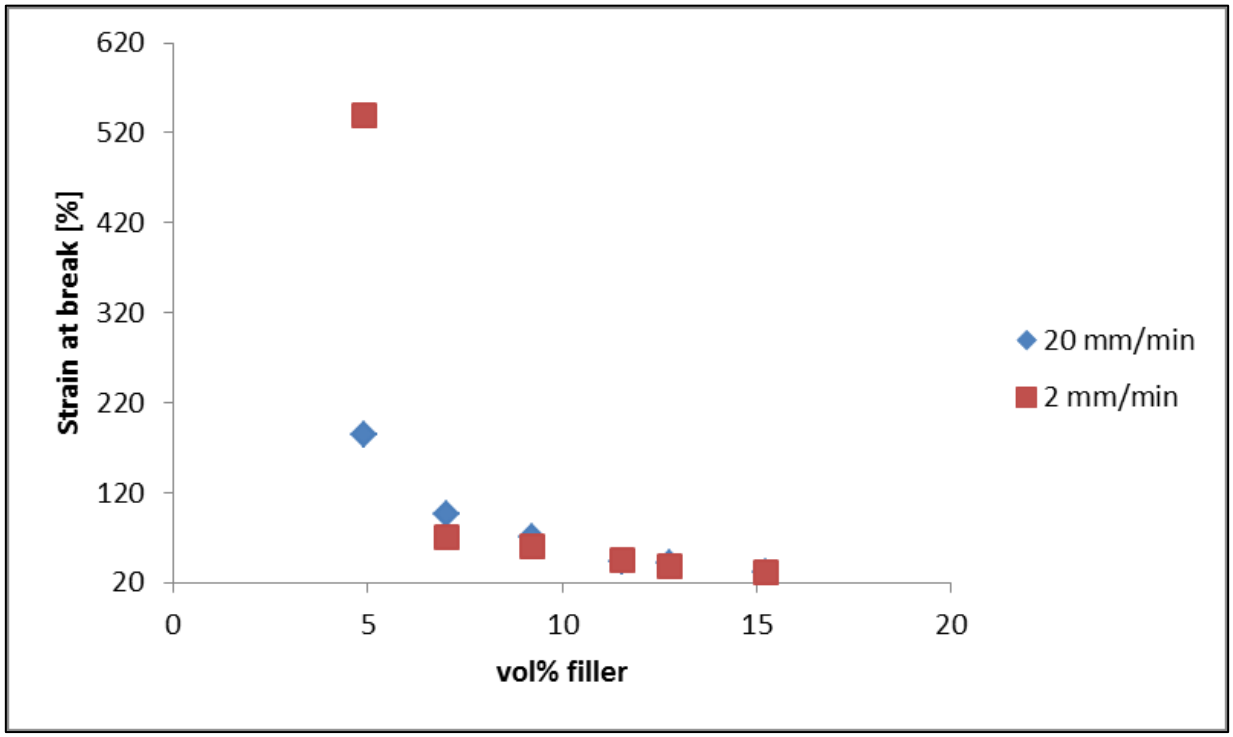

Figure 39. The strain at break (%) of the 80/20 GNP/LS – CB in EBA hybrid system as a function of the filler volume fraction (%), for the two different extrusion speeds, 2 mm/min and 20 mm/min.

Figure 39 indicates a higher value of the strain at break at 20 mm/min than at 2 mm/min, pointing to that the material was less brittle in the first case. This situation is not at hand at lower filler content (around 5 vol%). The strain at break related to an extrusion speed of 2 mm/min decreased dramatically from around 550% to around 30% at higher filler contents, where the two trends for the two different materials got closer each other.

Regarding the LS – CB/EBA composite, a reliable set of results for the strains at break was not obtained. Nevertheless, **Figure 40** shows the tensile modulus as a function of the filler volume content. There were no appreciable differences between the two extrusion speeds which perhaps can be attributed to a less efficient compounding step.

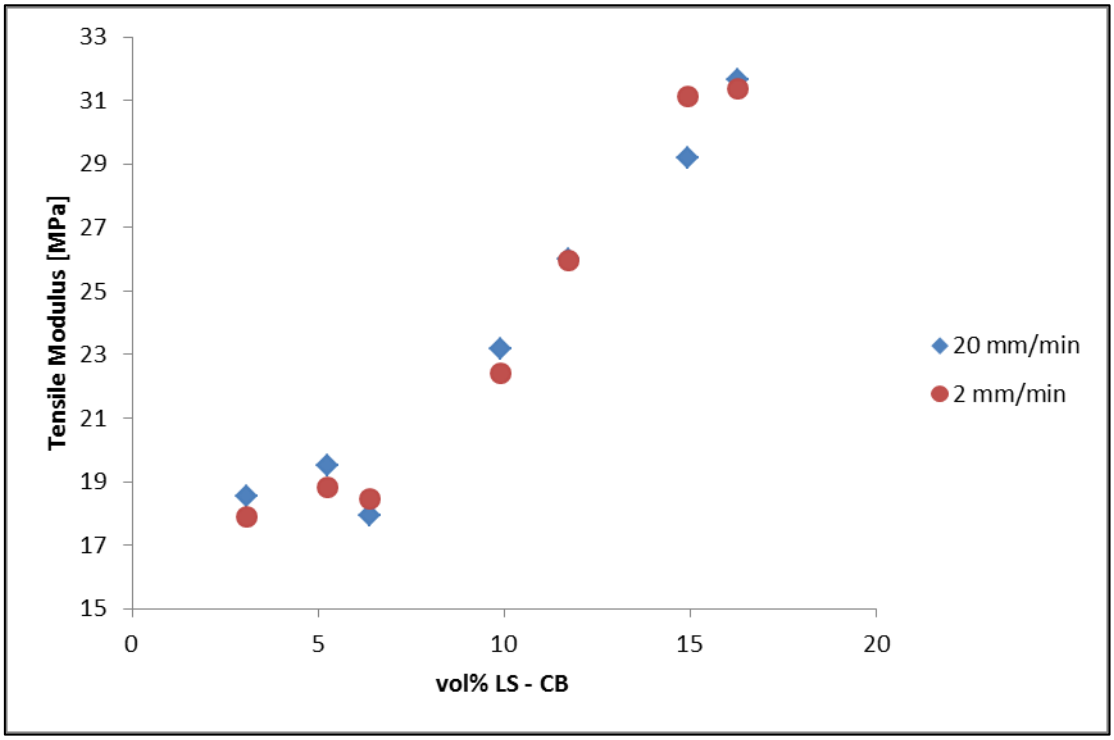

Figure 40. The tensile modulus (MPa) of the LS – CB in the EBA system as a function of the filler volume fraction (%), for the two different extrusion speeds, 2 mm/min and 20 mm/min.

5.4.1 The Halpin – Tsai and the Nielsen models

The tensile moduli obtained were analyzed using the Nielsen and the Halpin – Tsai models. In order to compare predictions of the models, characterized by different parameters depending on the aspect ratios (the Einstein coefficient K_E for Nielsen and L/d for Halpin – Tsai), a fixed value for the tensile modulus of the filler E_f was chosen. In case of the pure GNP/EBA system, **Figures 41** and **42** show the tensile modulus of the composite (in Pa) as a function of the filler volume fraction, and the predictions of the tensile modulus of the two models. The two figures refer to different extrusion speeds, 2 mm/min and 20 mm/min respectively. The tensile modulus of the matrix E_M was experimentally found to be 11.6 MPa at 2 mm/min, and 10.2 MPa at 20 mm/min.

A tensile modulus of the filler E_f equal to 36.5 GPa was here chosen, obtained as a fitting parameter from previous studies **[5, 23]**. This value is clearly much lower than could be expected, due to microstructural reasons. Indeed, graphene sheets are characterized by a tensile modulus of about 1 TPa in their plane. Graphite nanoplatelets (GNP) is composed of several sheet stacks, and they probably break up due to rupture of the Van der Waals interactions between the layered stacks when subjected to a tensile load. This takes place at significantly lower loads than would correspond to the graphitic carbon – carbon bonding within a graphite sheet. As a consequence, the GNP – particles exfoliate. The value taken as a reference for the tensile modulus of the filler is then referred to the direction of the first failure **[15].**

For Nielsen model, a maximum packing fraction φ_m of 0.3 was used, as obtained from rheological studies **[28]**. As a result of the data fitting, it was found that the Nielsen model gave a more reliable prediction of the experimental data than the Halpin – Tsai model, at both the extrusion speeds, even though it slightly overestimated the experimental values.

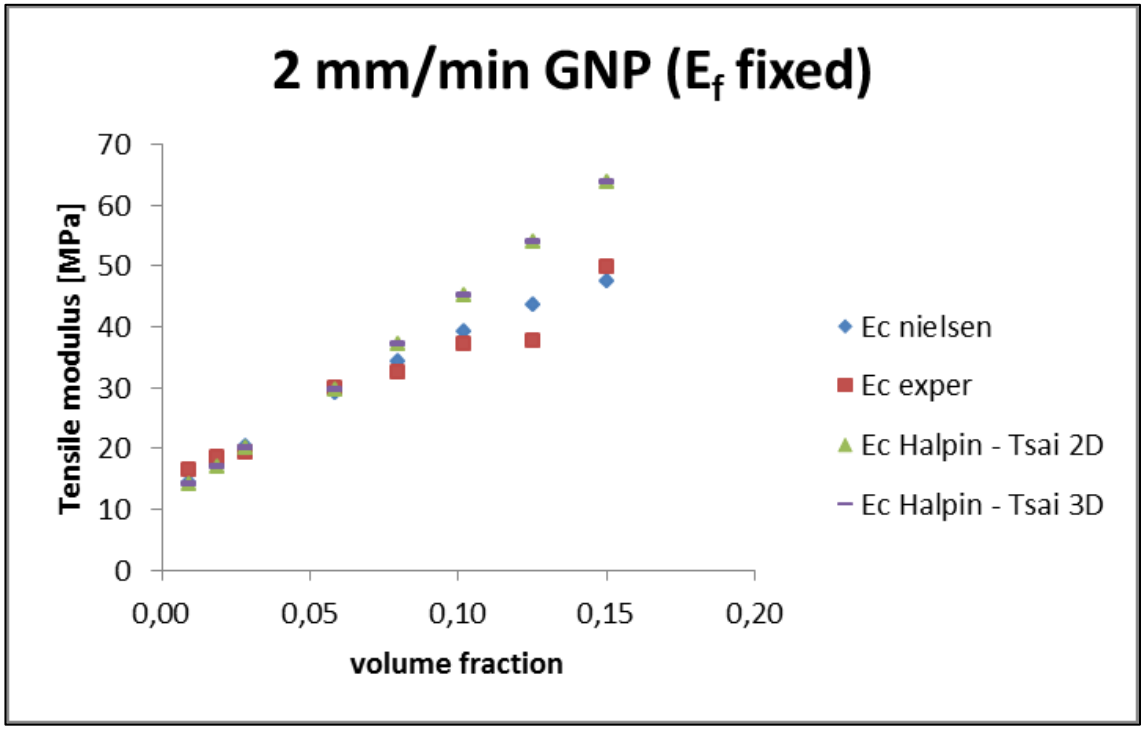

Figure 41. The tensile modulus of the pure GNP/EBA composite (MPa) as a function of the filler volume fraction at 2 mm/min, where experimental data are compared with the predictions of the Nielsen and the Halpin – Tsai models.

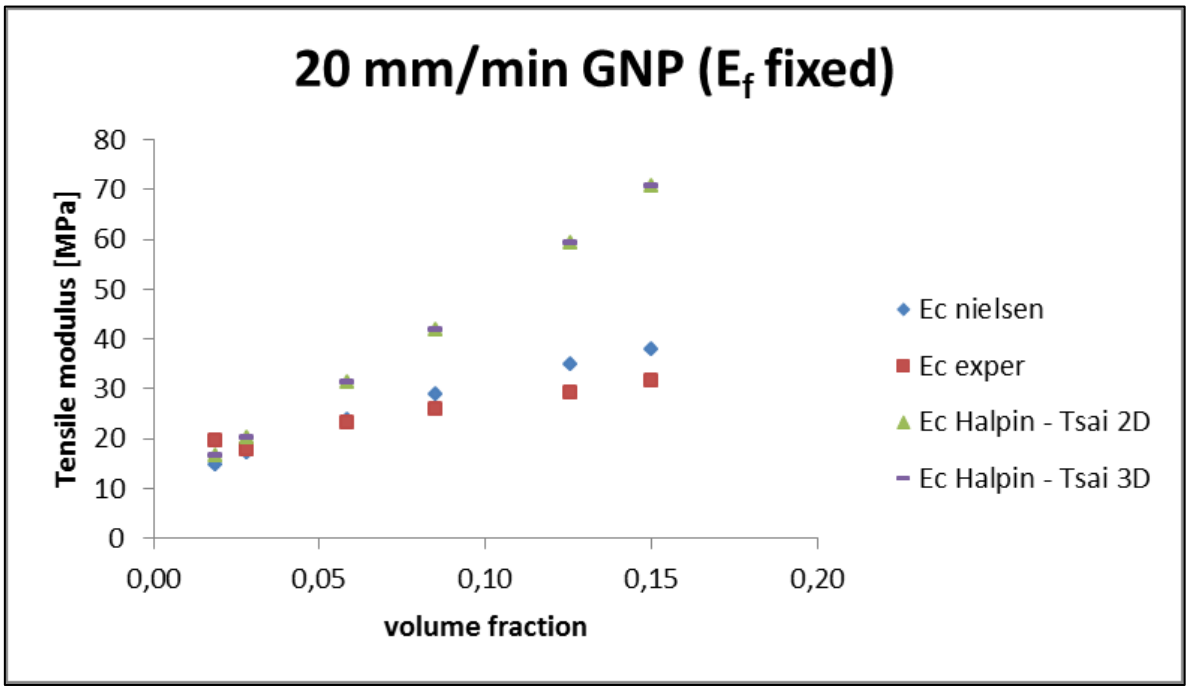

Figure 42. The tensile modulus of the pure GNP/EBA composite (MPa) as a function of the filler volume fraction at 20 mm/min, where experimental data are compared with the predictions of the Nielsen and the Halpin – Tsai models.

Another set of results were obtained with the LS – CB/EBA system, as shown in **Figures 43** and **44** (at 2 mm/min and 20 mm/min respectively).

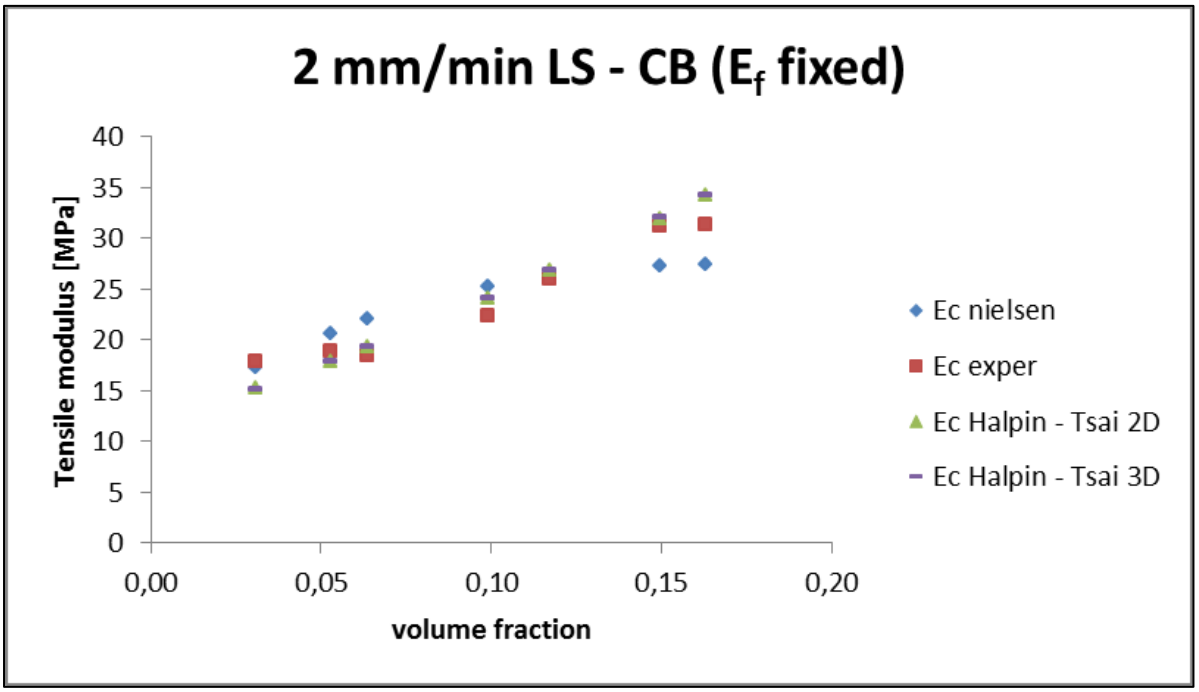

Figure 43. The tensile modulus of the LS – CB/EBA composite (MPa) as a function of the filler volume fraction at 2 mm/min, where experimental data are compared with the predictions of the Nielsen and the Halpin – Tsai models.

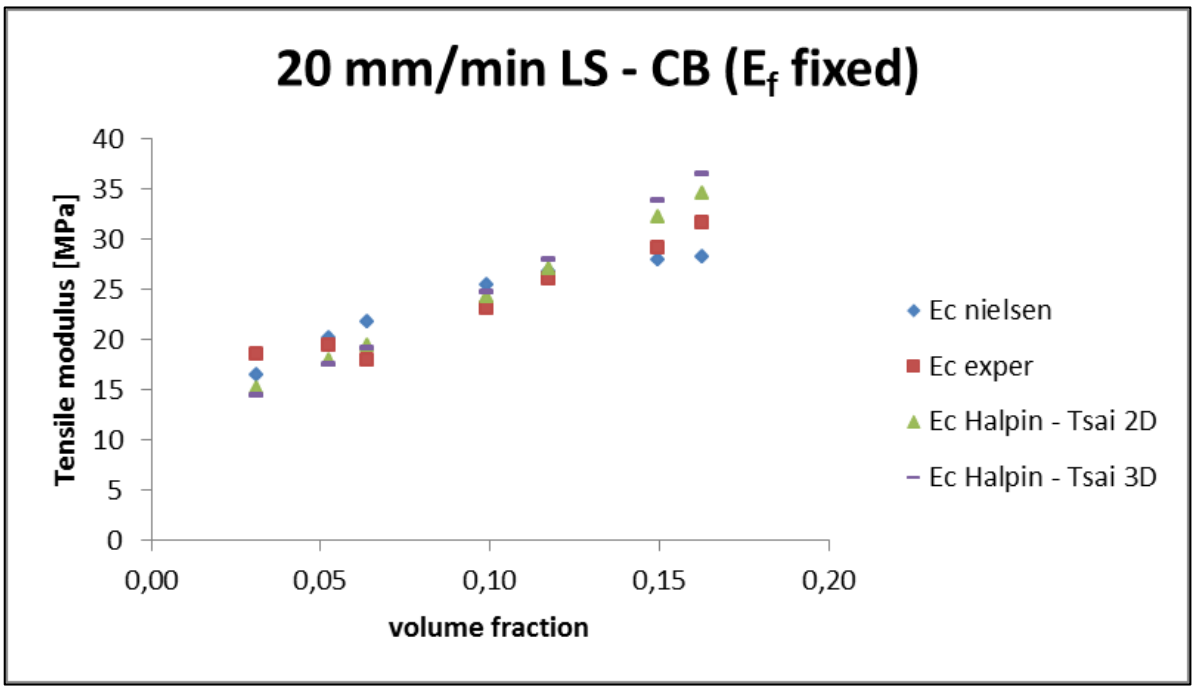

Figure 44. The tensile modulus of the LS – CB/EBA composite (MPa) as a function of the filler volume fraction at 20 mm/min, where experimental data are compared with the predictions of the Nielsen and the Halpin – Tsai models.

In this case, a tensile modulus of the filler E_f equal to 400 GPa was chosen, partly due to the unavailability of theoretical values or previous studies on this material (LS – CB). This value was simply chosen from the good results of the fitting procedure. For the Nielsen model, a maximum packing fraction φ_m of 0.2 was used, from the studies of **Gaxiola *et al.* [32]**, reported on by **Via *et al.* [5]**. There were only small differences between the predictions of the models as seen in **Figures 43** and **44**.

The 80/20 GNP/LS – CB – EBA hybrid system was analyzed using a tensile modulus of the filler E_f of 109.2 GPa, which gave the best fit to the experimental data. In this case, the maximum packing fraction φ_m for the Nielsen model was estimated using the rule of mixture (as a weighted average of the values for LS – CB/EBA and GNP/EBA composites), giving 0.28. As reported on **Figures 45** and **46** (at 2 mm/min and 20 mm/min, respectively), the Nielsen model predicted the experimental points better than Halpin – Tsai did, in parallel with the results for the pure GNP/EBA system.

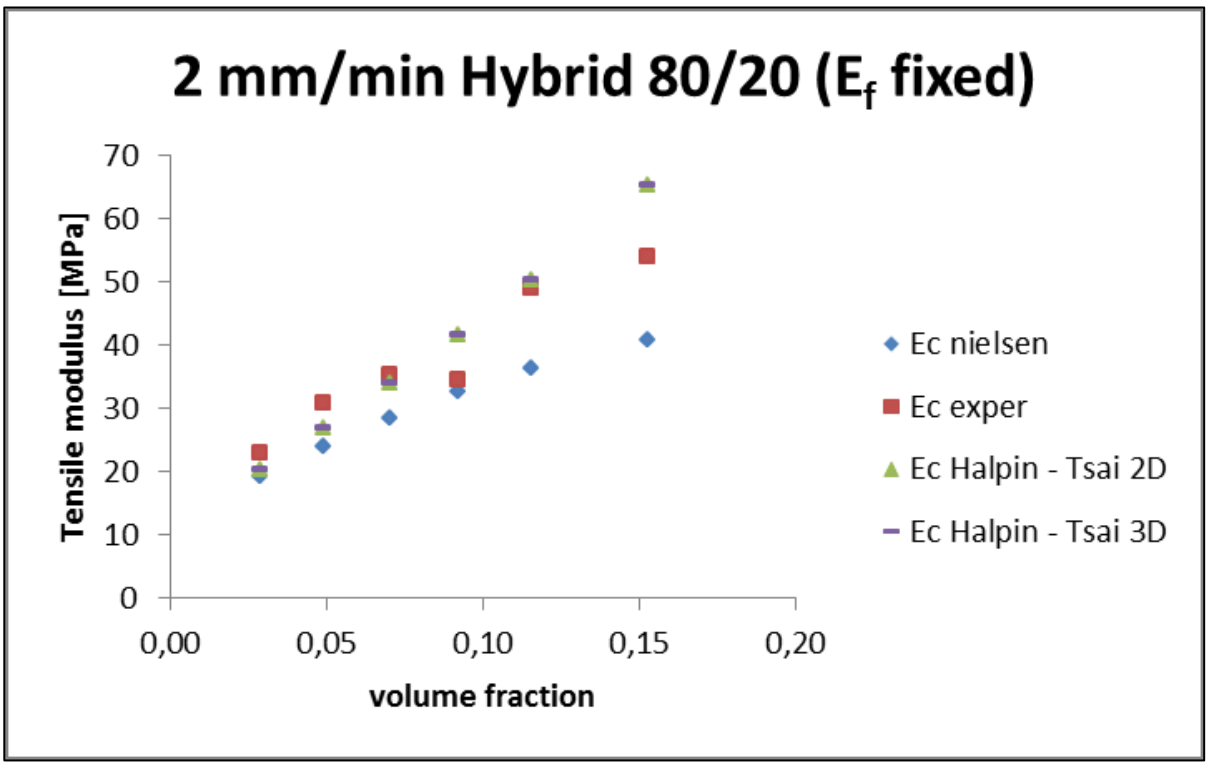

Figure 45. The tensile modulus of the 80/20 GNP/LS – CB in EBA composite (MPa) as a function of the filler volume fraction at 2 mm/min, where experimental data are compared with the predictions of the Nielsen and the Halpin – Tsai models.

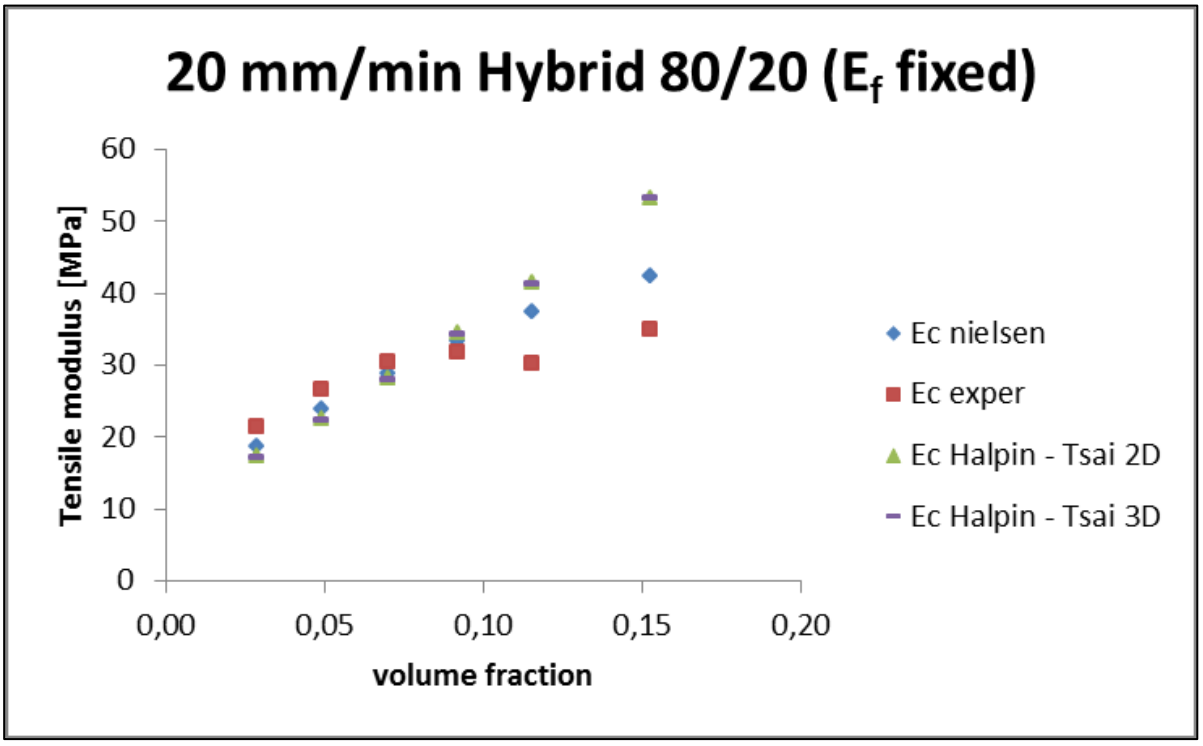

Figure 46. The tensile modulus of the 80/20 GNP/LS – CB in EBA composite (MPa) as a function of the filler volume fraction at 20 mm/min, where experimental data are compared with the predictions of the Nielsen and the Halpin – Tsai models.

In conclusion, the Nielsen model gave the best prediction of the experimental tensile modulus, especially for the GNP/EBA and the hybrid systems. Hence, more focus on this model applied to the GNP/EBA composite is worthwhile. In particular, the fitting step was performed varying alternatively the Einstein coefficient K_E and the tensile modulus of the filler E_f. In the first case, for the GNP/EBA composite, using a fixed value for E_f of 36.5 GPa (the reason of this choice is mentioned above), K_E equal to 30.8 for 2 mm/min and 27.2 for 20 mm/min were obtained. These values are much lower than the theoretical one of 173.3 assuming a diameter of the platelet D of 5 µm and a thickness t of 7 nm **[19]**. This mismatch can be attributed to the presence of agglomerates.

By fixing the Einstein coefficient at the theoretical value of 173.3, tensile moduli of the filler equal to 352.1 MPa at 2 mm/min and 271.3 MPa at 20 mm/min were found. The first value obtained is comparable with the one found by **Oxfall [19]**, equal to 425 MPa.

6. Conclusions

6.1 Microstructural studies

SEM micrographs of the composites 80/20 GNP/HS – CB (5.6 vol%) and pure GNP (9.1 vol%) in EBA were obtained, employing a JSM-7800F Thermal Field Emission Scanning Electron Microscope and a low vacuum JSM-6610 LV Scanning Electron Microscope. The samples were previously ion polished perpendicularly to the flow direction, with a broad ion beam, Gatan Iliont model 693.

The first system showed needlelike GNP structures, parallel to the surface of the specimen, oriented in the flow direction and with the tendency to agglomerate. At higher magnifications, the presence of platelets thinner than 20 nm, apparently isolated but actually connected to each other thanks to HS – CB particles was observed.

The orientation in the flow direction of the platelets, given by the extrusion step, was also found in the pure GNP (9.1 vol%) in EBA system.

6.2 Electrical properties

Electrical measurements were performed in order to determine the electrical conductivity of the strings extruded using a capillary viscometer (Ceast Rheoscope 1000 6742/00, Ceast SpA, Pianezza, Italy), employing two piston speeds, 2 mm/min (equivalent to a shear rate of 24.3 s^{-1}) and a higher one, 20 mm/min (meaning a shear rate of 243 s^{-1}). Their edges were painted with conductive silver paint and subsequently placed between two electrical clamps, in the two-point technique (*ASTM D257* standard test method). Three different voltage levels were used (depending on the electrical conductivity), and a digital multimeter (Fluke 8846A) revealed the average values of current I flowing through the specimens.

The electrical conductivity (S/cm) was determined as a function of the filler volume content for the systems made of EBA filled with GNP, LS – CB and several hybrids (80/20, 70/30 and 60/40 of GNP/LS – CB in EBA), obtained with an extrusion speed of 2 mm/min. The highest value of the percolation threshold belonged to the EBA/LS – CB system (11.7 vol% LS – CB), much higher than the one for the EBA/GNP system (7.4 vol% GNP). The addition of LS – CB to the latter system decreased the percolation threshold, due to the effectiveness of the LS – CB in creating a conductive network between the 2D oriented GNP (*synergistic effect*). It was also observed how a decrease of the LS – CB content in the hybrid systems ensured a lower percolation threshold: its lowest value was noted for the 80/20 and 70/30 systems (6.5 vol%).

The influence on the electrical properties of the orientation of the fillers in the flow direction has been also investigated. For this reason, two different extrusion speeds, 2 mm/min and 20 mm/min, were used. The electrical conductivity of the EBA/GNP system (9.1 vol%, 10.2 vol% and 11.4 vol%) manifested a decrease at the higher extrusion speed, because of the pronounced orientation of the graphite nanoplatelets. This can be interpreted in terms of poorer particle – particle interaction.

In a series of trials the electrical conductivity was measured for samples that had been subjected to up to three extrusion steps. The conductivity decreased with increasing number of such steps. This is probably due to a possible decrement of the conductive paths and interactions between GNP.

6.3 Rheological properties

The samples for the rheological measurements were produced as compression molded discs in a Bucher plastic press KHL 100. A stress-controlled rotational rheometer, Rheometrics SR 200, was used (180 ^{o}C, N_2 atmosphere), in order measure the storage modulus G'(MPa) and the loss modulus G''(MPa) as functions of the frequency (Hz), for three of the systems containing GNP, LS – CB and the 80/20 GNP/LS – CB in EBA hybrid system.

A first result was identified in the flattening out of the storage modulus G' at the lower frequencies (solid – like response, physically explained with the generation of a network between the platelets, which can ensure a mechanical reinforcement to the material). Theoretically, at low filler loadings, the loss modulus G'' is higher than G', meaning the viscoelastic behavior of the composite is mainly governed by the polymer matrix. This situation changed at increasing filler contents, with G' exceeding G'', at the rheological percolation threshold. This parameter for the LS – CB/EBA composite was found to be quite similar to the one for GNP/EBA system (7.4 vol% and 8 vol% respectively), which show a small difference between the rheological and the electrical percolation thresholds.

Only a weak correspondence for the LS – CB/EBA systems was noted. Indeed, the flattening out of G' began at 7 vol%, whereas the onset of the electrical conductivity was in the range 11.4 – 12 vol%. This remarkable result can be attributed to a less effective compounding step. The highest rheological percolation threshold belonged to 80/20 GNP/LS – CB in EBA hybrid, which also showed the lowest electrical percolation threshold: this could be useful in terms of combination of good electrical properties and manufacturing for the application in semiconductive layers for high voltage cables.

6.4 Mechanical properties

Uniaxial tensile tests were performed on samples of EBA with GNP, LS – CB and hybrid systems (1.9 – 15 vol% for the GNP systems, 3.1 – 16.3 vol% for the LS – CB materials and 2.9 – 15.3 vol% for the 80/20 hybrid), produced with two extrusion speed (2 mm/min and 20 mm/min). The tensile tests were also performed even on another GNP – EBA system, with a composition of 8 vol% of GNP, in order to analyze the influence of several steps of extrusion on the mechanical properties, in particular on the tensile modulus (in MPa) and the strain at break (%), as functions of the filler volume content.

Regarding the tensile modulus, it was noticed that an addition of 0.9 vol% of GNP to the polymer matrix ensured an increase by 43.23%, comparable to previous works **[2, 19]**.

For the pure GNP system, the extrusion speed had no significant influence on the tensile modulus for filler contents lower than about 10 vol%. At higher filler levels, the tensile modulus was higher for the samples that were produced at the higher speed, most likely to be associated with the more pronounced platelet orientation.

The strain at break decreased markedly at increasing GNP volume fractions (from around 350 – 550% at 2.8 vol% to around 30% at the highest volume content, 15 vol%).

The tensile modulus at the GNP/LS – CB in EBA hybrid system was higher for the samples produced at the lower extrusion speed, especially at higher filler contents. This was somewhat unexpected and could perhaps be associated with a less efficient compounding step. The strain at break was found higher for samples extruded at 20 mm/min than those obtained at 2 mm/min, indicating that the material was less brittle in the first case.

Regarding the LS – CB/EBA composite, the measurements of the tensile modulus provided scattered results, probably due to a less effective compounding step.

6.4.1 The Halpin – Tsai and the Nielsen models

The results of tensile moduli were analyzed using the Nielsen and Halpin – Tsai models, using a constant value for the tensile modulus of the filler E_f (36.5 GPa for the pure GNP/EBA system, as fitting parameter from previous studies **[5, 23]**, 400 GPa for LS – CB/EBA and 109.2 GPa for the 80/20 GNP/LS – CB in EBA hybrid system). The tensile modulus of the matrix E_M was experimentally found to be of 11.6 MPa at 2 mm/min, and of 10.2 MPa at 20 mm/min. For the Nielsen model, a maximum packing fraction φ_m of 0.3 was used for the pure GNP/EBA system, of 0.2 for LS – CB/EBA and 0.28 for the hybrid, determined using the rule of mixture.

In case of the pure GNP/EBA composite, it was found that the Nielsen model gave a better prediction of the experimental data than the Halpin – Tsai model, at both the extrusion speeds, even though it slightly overestimated the measured values. For the LS – CB/EBA system, only a very small difference between the predictions of the two models was noted. In parallel with the results for the pure GNP/EBA system, the hybrid behavior was better described by the Nielsen model.

7. References

[1] Green K., Theodore M., Abdalla M., Horton N., Noble A., Dean D., Fielding J., Miller S., "*Nanostructured coupling agents for multifunctional composites*", International SAMPE Technical Conference, (2008).

[2] Kim S., Do I., Drzal L. T., "*Multifunctional xGnP/LLDPE nanocomposites prepared by solution compounding using various screw rotating systems*", Macromolecular Materials and Engineering, 294 (3), 196-205 (2009).

[3] Potts J. R., Dreyer D. R., Bielawski C. W., Ruoff R. S., "*Graphene-based polymer nanocomposites*", Polymer, 52, 5-25 (2011).

[4] Sengupta R.; Bhattacharya M.; Bandyopadhyay S.; Bhowmick A. K., "*A review on the mechanical and electrical properties of graphite and modified graphite reinforced polymer composites*", Progress in Polymer Science, 36 (5), 638‑670 (2011).

[5] Via M. D., King J. A., Keith J. M., Miskioglu I., Cieslinski M. J., Anderson J. J., Bogucki G. R., "*Tensile Modulus Modeling of Carbon Black/Polycarbonate, Carbon Nanotube/Polycarbonate, and Exfoliated Graphite Nanoplatelet/Polycarbonate Composites*", Journal of Applied Polymer Science, 124, 2269–2277 (2012).

[6] Berkowitz B., Ewing R. P., "*Percolation theory and network modeling applications in soil physics*", Surveys in Geophysics, 19, 23–72 (1998).

[7] Wang M. J., Gray C. A., Reznek S. A., Mahmud K., Kutsovsky Y., "*Carbon black*", Kirk-othmer encyclopedia of chemical toxicology, 761-803 (2003).

[8] Baan R., "*Carcinogenic hazards from inhaled carbon black, titanium dioxide, and talc not containing asbestos or asbestiform fibers: Recent evaluations by an IARC monographs working group*", Inhal Toxicol, 19 (S1), 213-228 (2007).

[9] Herd C. R., McDonald G. C., Hess W. M., "*Morphology of carbon-black aggregates. Fractal versus Euclidean geometry*", Rubber Chemistry and Technology, 65 (1), 107-129 (1992).

[10] Corry B. R., "*Overview of carbon black in plastics applications*", Industrial Minerals, 26-32 (1985).

[11] Stankovich S., Dikin D. A., Dommett G. H. B., Kohlhaas K. M., Zimney E. J., Stach E. A., Piner R. D., Nguyen S. T., Ruoff R. S., "*Graphene-based composite materials*", Nature, 442, 282-286 (2006).

[12] Kim H., Macosko C. W., "*Morphology and Properties of Polyester/Exfoliated Graphite Nanocomposites*", Macromolecules, 41, 3317-3327 (2008).

[13] Li B., Zhong W-H, "*Review on polymer/graphite nanoplatelet nanocomposites*", Journal of Material Science, 46, 5595-5614 (2011).

[14] Falcao E. H. L., Blair R. G., Mack J. J., Viculis L. M., Kwon C. W., Bendikov M., Kaner R. B., Dunn B. S., Wudl F. , "*Microwave exfoliation of a graphite intercalation compound*", Carbon, 45 (6) , 1367-1369 (2007).

[15] Hernandez Y., Nicolosi V., Lotya M., Blighe F. M., Sun Z., De S., et al., "*High-yield production of graphene by liquid-phase exfoliation of graphite*", Nature Nanotechnology, 3 (9), 563-568 (2008).

[16] Lotya M., Hernandez Y., King P. J., Smith R. J., Nicolosi V., Karlsson L. S., et al., "*Liquid Phase Production of Graphene by Exfoliation of Graphite in Surfactant/Water Solutions*" Journal of the American Chemical Society, 131 (10), 3611-3620 (2009).

[17] Lu J., Yang J. X., Wang J., Lim A., Wang S., Loh K. P., "*One-pot synthesis of fluorescent carbon nanoribbons, nanoparticles, and graphene by the exfoliation of graphite in ionic liquids*", ACS Nano, 3 (8), 2367-2375 (2009).

[18] Park S., Ruoff R. S., "*Chemical methods for the production of graphenes*", Nature nanotechnology, 4, 217-224 (2009).

[19] Oxfall H., "*Manifacturing and Characterization of Filled Polymeric Systems – Powder Injection Moulding Fedstocks and Graphite Nanoplatelet Based Nanocomposites*", Department of Materials and Manufacturing Technology – Chalmers University of Technology, (2013).

[20] Kotsilkova R., "*Thermoset Nanocomposites for Engineering Applications*", Smithers Rapra Technology Limited: Shawbury, (2), 25-54 (2007).

[21] Spikowski J. M., Gibbins C., Shoemaker C. L., Kunzelman J., "*Variability in standard two-probe and four-probe electrical resistivity measurements of carbon nanotube composites*", Antec, 1-7 (2011).

[22] Halpin J. C., "*The Halpin-Tsai Equations: A Review*", Polymer Engineering and Science, 16 (5), 344-352 (1976).

[23] King J. A., Klimek D. R., Miskioglu I., Odegard G. M., "*Mechanical Properties of Graphene Nanoplatelet/Epoxy Composites*", Journal of Applied Polymer Science, 1-7 (2012).

[24] Kanagaraj S., Varanda F. R., Zhiltsova T. V., Oliveira M. S. A., Simões J. A. O., "*Mechanical properties of high density polyethylene/carbon nanotube composites*", Composites Science and Technology, 67, 3071–3077 (2007).

[25] Li W., Dichiara A., Bai J., "*Carbon nanotube–graphene nanoplatelet hybrids as high-performance multifunctional reinforcements in epoxy composites*", Composites Science and Technology, 74, 221–227 (2013).

[26] ASTM D 257 - 07, "*Standard Test Methods for DC Resistance or Conductance of Insulating Materials*", (2007).

[27] Wei T., Song L., Zheng C., Wang K., Yan J., Shao B., Fan Z., "*The synergy of a three filler combination in the conductivity of epoxy composites*", Materials Letters, 64, 2376-2379 (2010).

[28] King J. A., Via M. D., Morrison F. A., Wiese K. R., Beach E. A., Cieslinski M. J., Bogucki G. R., "*Characterization of exfoliated graphite nanoplatelets/polycarbonate composites: electrical and thermal conductivity, and tensile, flexural, and rheological properties*", Journal of Composite Materials, 46(9), 1029–1039 (2011).

[29] King J. A., Via M. D., King M. E., Miskioglu I., Bogucki G. R., "*Electrical and Thermal Conductivity and Tensile and Flexural Properties: Comparison of Carbon Black/Polycarbonate and Carbon Nanotube/Polycarbonate Resins*", Journal of Applied Polymer Science ,121, 2273–2281 (2011).

[30] Zheng Q., Song Y., Wu G., Song X., "*Relationship between the Positive Temperature Coefficient of Resistivity and Dynamic Rheological Behavior for Carbon Black-Filled High-Density Polyethylene*", Journal of Polymer Science – Part B: Polymer Physics, 41, 983–992 (2003).

[31] Stråat M., Toll S., Boldizar A., Rigdahl M., Hagström B., "*Melt Spinning of Conducting Polymeric Composites Containing Carbonaceous Fillers*", Journal of Applied Polymer Science, 119, 3264–3272 (2011).

[32] Gaxiola D. L., Jubinski M. M., Keith J. M., King J. A., Miskioglu I., "*Effects of Carbon Fillers on Tensile and Flexural Properties in Polypropylene-Based Resins*", Journal of Applied Polymer Science ,118, 1620–1633 (2010).